Supercritical Fluids for the Fabrication of Semiconductor Devices: Emerging or Missed Opportunities?

Alvin H. Romang and James J. Watkins*

Polymer Science and Engineering Department, University of Massachusetts—Amherst, Amherst, Massachusetts 01003

Received July 22, 2009

Contents

1. Introduction 459
2. Supercritical Fluids as Processing Media for Nanostructured Devices 460
3. Applications in Device Fabrication 461
3.1. Metal and Metal Oxide Deposition 461
3.2. Metal and Metal Oxide Etching in Supercritical Fluids 467
3.3. Photoresist Processing and Development 468
3.4. Wafer Cleaning and Photoresist Stripping 470
3.5. Ordered Porous ULK Films 471
3.6. Directly Patterned Dielectrics in Four Process Steps 474
3.7. Surface Modification of Nanoporous Substrates 475
4. Conclusions 475
5. Acknowledgments 476
6. References 476

1. Introduction

Next generation semiconductor devices and evolving opportunities in nanoelectronics present new challenges for fabrication technology. These include patterning and structure generation to define the smallest features, the deposition of metals, metal oxides, and other functional layers within challenging topographies, and development of the associated integration steps necessary to create working devices. Implementation of emergent technical solutions, however, is also subject to economic realities that require high volume process tools, reliability, and low cost per device layer.

Changes in semiconductor process technology have to date largely been driven by the continued downscaling of device features to increase transistor density. Leading edge microprocessors are currently in production at the 45 nm device node. Device dimensions approaching 22 nm will be realized withinin the next several years. As manufacturing moves to smaller and smaller features, it is necessary to re-evaluate process technology and decide if evolutions in current methods are sufficient or if technical and/or economic considerations will mandate change. Semiconductor fabrication relies on a combination of gas (or vapor) based techniques and liquid phase processing. Each has its advantages. Gas phase techniques allow for dry processing, complete wetting of surfaces, and the absence of surface tension, which in turn allows facile transport of reagents into confined geometries. Vapor phase transport of reagents and processing aids, however, are subject to species volatility

* Corresponding author. E-mail: watkins@polysci.umass.edu.

Alvin H. Romang was born in Makassar, Indonesia. He completed his undergraduate degree in chemical engineering at the University of Wisconsin—Madison in 2004. He received the Meyer Award in 2003 for academic excellence. His current doctoral research involves the synthesis of mesoporous silicas for low dielectric materials in supercritical CO_2 under the supervision of Prof. James J. Watkins. Other previous areas of work include block copolymer blends and microemulsion formation in supercritical CO_2. He will complete his Ph.D. in chemical engineering at the University of Massachusetts—Amherst in 2009.

constraints. Liquid phase processes have the advantage of species transport in solution, but the presence of the liquid phase can give rise to contamination issues, sluggish mass transport, and difficulties such as pattern collapse for the smallest device features. The latter arises from surface tension and associated capillary forces. These limitations are especially relevant for processing and fabrication at the nanoscale.

In this review, we describe the use of supercritical fluids (SCFs) such as carbon dioxide as a scalable process alternative to enable the fabrication of nanostructured devices. The properties of supercritical fluids are detailed below, but in the simplest sense they represent a state of matter that is intermediate between liquids and gases.[1] Their liquid-like densities can enable the dissolution and transport of reagents and other species while their gas-like transport properties, including low viscosities, high diffusivities, and the absence of surface tension, are well suited for processing nanostructures.[2] From that basic viewpoint, the combination of desirable properties of SCFs is compelling for the fabrication of nanostructure devices. If one were to design a fabrication strategy for this purpose without a long history of liquid and gas phase processing in industry, it would be a logical place to start. Because it is not the starting point, the case for implementation of an SCF process, or any new process technology, must be compelling. Does the technology provide a technical or economic advantage that cannot be realized

10.1021/cr900255w © 2010 American Chemical Society
Published on Web 12/17/2009

Jim Watkins is a Professor of Polymer Science and Engineering and Director of the Center for Hierarchical Manufacturing, a National Science Foundation Nanoscale Science and Engineering Center (NSEC) at the University of Massachusetts—Amherst. Professor Watkins received his B.S. and M.S. degrees in Chemical Engineering from the Johns Hopkins University and his Ph.D. in Polymer Science and Engineering from the University of Massachusetts. Between his graduate degrees, Dr. Watkins was a Senior R&D Engineer at Phasex Corp., Lawrence, MA. He joined the Chemical Engineering faculty at UMass in 1996 and the Polymer Science and Engineering Faculty in 2005. His research interests include nanotechnology and materials processing in supercritical fluids. He is the recipient of the NSF Career Award, the Camille Dreyfus Teacher—Scholar Award, and a David and Lucile Packard Foundation Fellowship for Science and Engineering.

through the evolution of existing techniques? Here we attempt to provide a perspective on this question.

Although supercritical carbon dioxide processing can be viewed as a "greener" alternative to other techniques, we do not place primary focus on this point.[3−8] Should SCF technology be implemented in industry, it is a welcome benefit that will follow. What is clear is that interest in the field, particularly in the area of cleaning and photoresist stripping, led to the development of full wafer process cluster tools that can be integrated into production lines.[5,9] These applications are among the most difficult for SCF carbon dioxide relative to its intrinsic physicochemical properties. In particular, they require very high solvent volumes, high pressures, and additives to promote the solubility of materials that exhibit a poor native solubility in CO_2. Moreover, the competing alternatives are relatively inexpensive and effective.

Applications development for SCF cleaning and photoresist stripping has been widely reviewed and is not the primary focus of this article.[3−5,7−9] Instead, we concentrate on areas that are particularly well-positioned to take advantage of the unique properties of SCFs to deliver significant performance improvements and in at least one case, lower cost. These processes include conformal metal and metal oxide deposition, the preparation of ultra low *k* dielectrics, directly patterned dielectrics, and nanostructured metal oxide films, and the design and implementation of materials and processes for high resolution lithography. These applications generally involve low solvent volumes, relatively low pressures, and address technical needs in areas that can support reasonable process cost. These are also applications that benefit from the fact that CO_2 is a relatively inert solvent for reactions and process chemistry. Our group is involved in several of these activities, so even though we have attempted to be comprehensive in the areas we discuss, it is reasonable to state that our views and selection of topics is influenced by our experience and perspective.

Table 1. Critical Parameters of Selected Solvent Systems[19]

solvent	critical temp (°C)	critical pressure (bar)
carbon dioxide	30.98	73.8
ethane	32.18	48.7
propane	96.68	42.5
hexane	324.67	30.3
water	373.95	220.6

Although our primary focus is on device fabrication using Si wafer platforms, many of the techniques are relevant to materials processing needs in other fields including catalysis, energy conversion, and separation science. Previous reviews take a much broader view of materials chemistry and processing in SCFs, and we refer the reader to these for a broader perspective on the technology.[2,10−18] Here, we begin with the properties of SCF media and the rationale for their use at the nanoscale and then move toward potential applications.

2. Supercritical Fluids as Processing Media for Nanostructured Devices

A supercritical fluid is simply a material heated and compressed beyond its critical temperature (T_c) and pressure (P_c). CO_2 is the fluid of choice for many applications because it is nonflammable, nontoxic, and exhibits easily accessible critical parameters ($P_c = 73.8$ bar, $T_c = 30.98$ °C); however, other fluids are used as specific applications dictate (Table 1).[19] As a gas is compressed above its critical point, it does not cross a phase transition but rather exhibits a continuous increase in density. As shown in Figure 1a for carbon dioxide, density can be controlled through variations in system pressure and temperature and can meet or exceed that of liquid solvents.[19] By comparison, a vapor held below its critical temperature will condense at its vapor pressure yielding a liquid phase. In supercritical fluids, other physicochemical properties, including viscosity, are also pressure-dependent and generally intermediate to those of the liquid and gaseous states (Table 2). A comparison of the surface tensions of water, hexane, and liquid CO_2 as a function of temperature at saturation is shown in Figure 1b.[19] At temperatures above the critical point, surface tension vanishes.

Liquid-like densities enable the dissolution of many organic and organometallic compounds in SCFs that can serve as precursors and reagents for subsequent processing steps. For example, Figure 1c shows the solubility of nickelocene in CO_2 at three temperatures as a function of density.[20] The combination of precursor and reagent solubility, favorable transport properties, and the absence of surface tension enables solution-based chemistry and processing in a supercritical medium that behaves much like a gas. This provides a situation that is ideal for the fabrication of nanostructured components. For example, SCF-based deposition, etching, cleaning, and surface modification can be carried out within the smallest features without damage due to capillary forces, limitations to wetting or flow in confined geometries, or concerns about residual solvent contamination. SCF processing with light gases such as CO_2 can be considered a "dry" process, as the solvents dissipate completely upon depressurization. Moreover, transport in solution

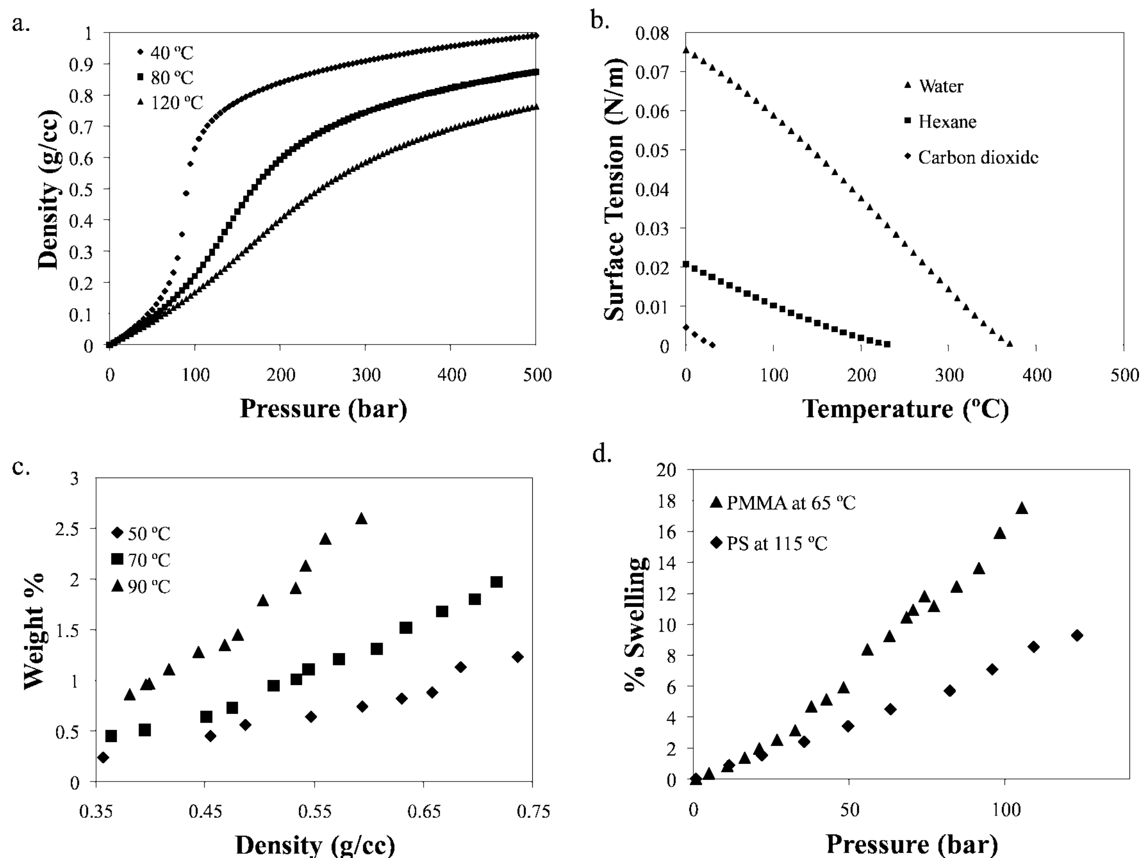

Figure 1. Properties of supercritical fluid systems. (a) Density of CO_2 as a function of pressure for isotherms at 40, 80, and 120 °C.[19] (b) Surface tension of water, hexane, and liquid carbon dioxide as a function of temperature at saturantion. Surface tension for all fluids vanishes at the critical points.[19] (c) Solubility of nickelocene in supercritical CO_2 as a function of pressure at 50, 70, and 90 °C.[20] (d) Swelling of polystyrene (PS) at 115 °C and poly(methyl methacrylate) (PMMA) at 65 °C as a function of pressure.[21]

Table 2. Comparison of Selected Properties of Supercritical Fluids to Those of Liquids and Gases

	liquid	supercritical fluid	gas
density (g/cm^3)	1	0.1−1	10^{-3}
viscosity (Pa·s)	10^{-3}	10^{-4}−10^{-5}	10^{-5}
diffusivity (cm^2/s)	10^{-5}	10^{-3}	10^{-1}
surface tension (dyn/cm)	20−50	0	0

eliminates precursor and reagent volatility concerns that often prove to be limiting in vapor-phase processes.

The interaction of polymers with SCFs, particularly carbon dioxide, also provides unique opportunities for the preparation of nanostructured materials using a bottom-up approach in which self-assembled polymer films serve to template the device. While most polymers are insoluble in supercritical CO_2, pressure-mediated adjustments in density can be used to precisely control the dilation of polymers and the distribution of reactants between an insoluble polymer and the fluid media. The equilibrium-limited sorption of CO_2 in polystyrene and poly(methyl methacrylate) as a function of pressure and temperature is shown in Figure 1d.[21] The sorption of modest amounts of the fluid can significantly depress the glass transition temperature[22,23] and increase the diffusivity of small molecules within the polymer,[24] thereby enabling efficient reactions within the dilated polymer phase.[25] As detailed later, deposition reactions within polymer templates dilated in CO_2 yield ultralow k and directly patterned dielectrics. The lack of solubility of most polymers in neat CO_2[18,26] also represents a challenge for photoresist stripping.

3. Applications in Device Fabrication

3.1. Metal and Metal Oxide Deposition

The deposition of metal and metal oxide films is essential for the fabrication of interconnects, electrodes, and barriers for integrated devices. As critical device dimensions shrink and aspect ratios increase, conformal deposition of metal and metal oxide films within device features is increasingly difficult. Rapid and efficient processes, for example, could enable the fabrication of 3-D capacitor structures. While vapor-phase techniques such as chemical vapor deposition (CVD) and atomic layer deposition (ALD) are ideally suited for these applications in principle, their implementation has often been hindered by secondary issues such as precursor volatility, deposition rate, step coverage, film quality, and adhesion. In CVD, the realization of acceptable step coverage in complex features can be problematic due to low vapor phase precursor concentrations resulting from limited precursor volatility. Low concentrations in turn lead to mass transport limited kinetics and consequently nonuniform deposition profiles in deep features. By contrast ALD provides excellent step coverage via deposition of submonolayer quantities of oxide or metal in each reaction cycle. However, the number of reactive cycles required to generate films thicker than a few nanometers and the associated process time is an issue for many applications that require thicker films. Moreover, like CVD precursors, ALD precursors are subject to volatility constraints. A process that offers excellent step coverage and a single step, high rate deposition

Table 3. Summary of Metal and Metal Oxide Films Deposited by Supercritical Fluid Transport Chemical Deposition and Their Deposition Conditions

film	precursor	solvent	deposition temp (°C)	substrate	ref
Al	$Al(hfa)_3$	pentane	680	Si, SiO_2	27
Ag	Ag triflate	diethyl ether	600	Si, SiO_2	27
	AgI	acetone	600	Si, SiO_2	27
Cr	$Cr(acac)_3$	acetone	800	Si, SiO_2	27
Cu	$Cu(oleate)_2$	pentane	740	Si, SiO_2	27
	$Cu(tmhd)_2$	N_2O	700	Si	27
In	$In(acac)_3$	CO_2	600	Si, SiO_2	27
Ni	$Ni(tmhd)_2$	pentane	600	Si, SiO_2	27
Pd	$Pd(tmod)_2$	pentane	600	Si, SiO_2	27
Y	$Y(tmhd)_3$	N_2O (H_2)	687	Si	27
Zr	$Zr(tfa)_4$	diethyl ether	600	Si, SiO_2	27
InP	$In(acac)_3$, Cp_3In, CpIn, $[(C_6H_4)CH_2N(CH_3)_2]_3In$ + $(C_6H_5)_3P$, $(C_6H_{11})_3P$	CO_2, Xe, C_2F_6	550−620	InP	28
Al_2O_3	$Al(hfa)_3$	N_2O	100	Si, SiO_2	27
Cr_2O_3	$Cr(hfa)_3$	N_2O	100	Si, SiO_2	27
CuO	$Cu(tmhd)_2$	N_2O	100	Si, SiO_2	27
SiO_2	$Si(OC_2H_5)_4$	N_2O	100	Si, Al, cast acrylic	27
BPSG	$Si(OC_2H_5)_4$ + $P(OC_2H_5)_4$ + $B(OC_2H_5)_4$	N_2O	100	Si, Al	27
$YBa_2Cu_3O_{7-x}$	$Y(tmhd)_3$ + $Ba_5(tmhd)_9(H_2O)_3OH$ + $Cu(tmhd)_2$	pentane	800	Si, SiO_2	27

scheme would represent a significant step forward. Deposition from supercritical fluid media offers such a potential.

Using a process called supercritical fluid transport and chemical deposition (SFT-CD), Sievers and co-workers were among the first to use the solubility of organometallics in SCFs for the development of process strategies to mediate precursor volatility constraints in CVD processes.[27] In this approach, precursor aerosols were produced by preparing solutions of precursors in a supercritical fluid, followed by rapid expansion of the supercritical solvent (RESS) to atmospheric pressure upstream of a CVD reactor. The precursor aerosol was directed onto a heated target substrate and pyrolized, oxidized, or reduced at ambient pressure to yield metal, metal oxide, and mixed oxide systems. This scheme provides an efficient means of delivering a precursor aerosol to a conventional CVD reactor. The process was used to produce films containing Al, Ag, Cr, Cu, In, Ni, Pd, Y, and Zr. A variation of the SFT-CD approach was used to produce metal oxide such as Al_2O_3, Cr_2O_3, CuO, SiO_2, and boron-doped and phosphorus-doped SiO_2 films by expansion from solutions of N_2O. It should be noted that the use of N_2O, a strong oxidizer, requires extreme care.[27] Popov et al. used a similar method to generate InP films.[28] A summary of a number of films produced by SFT-CD is provided in Table 3. While these approaches offer a useful means of generating aerosols of low-volatility precursors, deposition and film formation occurs at conditions similar to those of CVD and therefore does not overcome issues related to poor step coverage in confined geometries.

Recently, we and others have demonstrated that device-quality, conformal films can be achieved by carrying out the depositions at high pressure in the presence of solutions of the precursor in supercritical fluids. The process, called supercritical fluid deposition (SFD), involves the deposition of metals and metal oxide films by reaction of suitable precursors in an SCF solution at a heated surface within a high-pressure reactor (see Figure 2).[29,30] Reactive deposition within SCFs can be viewed as a hybrid of solution and vapor phase techniques that exploits the desirable properties of each. Like electroless plating, SFD is solution based, but the transport properties of SCFs, which are more akin to those of a gas, afford distinct advantages that are typically associated with CVD including low viscosity, rapid diffusion,

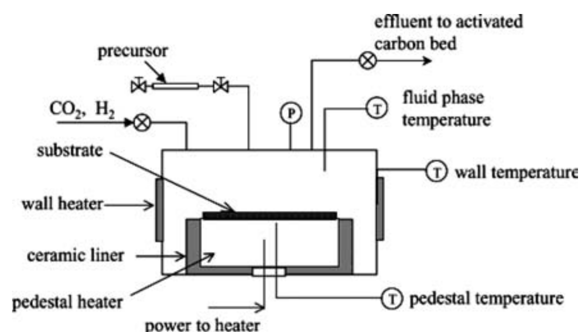

Figure 2. Schematic of a cold wall supercritical fluid deposition reactor.[38] Reprinted with permission from ref 38. Copyright 2004 American Chemical Society.

and the absence of surface tension. The enabling distinction between SFD and CVD is the mode of precursor transport. In CVD, the limited volatility of suitable precursors, including organometallics, leads to low vapor phase concentrations and mass transfer limited reactions that preclude uniform depositions. In SFD, precursor concentrations in supercritical CO_2 solution are up to 3 orders of magnitude greater than CVD. The solubility of nickelocene in CO_2 is shown in Figure 1c. For comparison, Figure 3 shows the vapor pressure of nickelocene as a function temperature.[31,32] The inset compares concentrations in terms of volumetric density for nickelocene dissolved in CO_2 relative to concentrations at its vapor pressure. The enhancement is greater than 3 orders of magnitude. Such high precursor concentrations can yield reaction rate limited deposition kinetics and conformal coverage at high deposition rate.[33−35]

Typical precursors for SFD include metallocenes and metal diketonates. Many common CVD precursors are sufficiently soluble in CO_2 and provide a suitable starting point for screening potential chemistries. For metal deposition, reduction of precursor is commonly performed using hydrogen or alcohol,[36] which are miscible with supercritical CO_2 above the mixture critical points. This approach has been used for the deposition of high-purity metal films including Ag, Au, Co, Cu, Ir, Ni, Pd, Pt, Rh, and Ru.[34,36−50] The phase behavior of the H_2/CO_2 system[51] and alcohol/CO_2 systems[52,53] are described in the literature. H_2 assisted reductions of precursors to yield metal films in our laboratories are conducted at H_2 concentrations in CO_2 well below the lower explosion

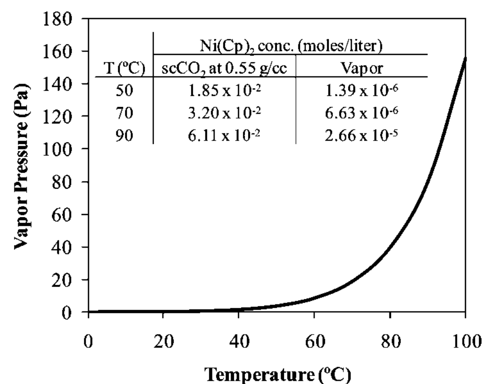

Figure 3. Vapor pressure of nickelocene at different temperature, calculated with Clausius−Clapeyron equation from data by Brissonneau et al.[31,32] Inset is a comparison of nickelocene concentrations between the vapor phase and the solubility limits in $scCO_2$ at a CO_2 density of 0.55 g/cm^3.[20]

limit (LEL) of H_2 in air (4%). Table 4 provides a summary of deposition conditions for a number of films.

Cu deposition is of considerable interest due to its relevance to interconnect structures, and thus it has been studied in the greatest detail. Watkins and co-workers reported the single step, conformal deposition of high purity Cu films by the reduction of Cu(I) and Cu(II) β-diketonates including hexafluoroacetylacetonate 2-butyne copper (Cu(I)-(hfac)(2-butyne)) and 2,2,6,6 tetramethyl-3,5-heptanedionato copper (Cu(tmhd)$_2$) in a high pressure, cold wall SFD reactor (see Figure 4a). Cu depositions are typically carried out at pressures between 100 and 250 bar and substrate temperatures between 200 and 300 °C. For reductions with hydrogen at temperatures above 225 °C, seed layers are not required on dielectric or barrier surfaces, yielding a single-step method for feature fill. The use of a cold-wall pressure vessel, in which the substrate is mounted on a heated stage, provides a means to localize the deposition to the desired surface. Heat and mass transfer in these reactors have been simulated by computational fluid dynamics to provide heuristics for scale up.[56] Deposition rates are on the order of 30 nm/min at typical conditions.[54] These rates are comparable to those of Cu CVD using hydrogen assisted reduction of copper(II) hexafluoroacetylacetonate (10−100 nm/min).[55]

Cu films produced by SFD exhibit excellent purity. Figure 5 shows secondary ion mass spectroscopy (SIMS) data for Cu films deposited at 300 °C on TaN wafers from solutions of Cu(tmhd)$_2$ in CO_2 using either ethanol or H_2 as the reducing agent. The analysis indicates that oxygen and carbon concentrations in films deposited at 300 °C using ethanol are on the order of 0.1% or less. At the same temperature, films deposited using H_2 showed oxygen and carbon concentrations an order of magnitude lower. One advantage of the SCF route for depositions is the elimination of the need for fluorinated precursors, which in turn obviates concerns regarding fluorine contamination of film surfaces and its deleterious impact on performance, contamination, and adhesion. The high purities of the films produced by SFD result in excellent electrical properties (resistivity $\sim 2.0\ \mu\Omega$ cm), which easily meets integration requirements.[29]

A kinetic analysis of the copper deposition process was performed by Zong et al. and revealed a zero-order reaction-rate dependence on precursor concentration for all but the most dilute reaction conditions.[35] Similar trends were reported by Kondoh at intermediate temperatures using a different precursor system for Cu.[34] The ability to maintain zero-order kinetics over a wide range of concentrations facilitates exceptional step coverage, as concentration gradients that may arise in the trench are insufficient to cause a transition out of the surface reaction-rate-limited regime. Thus, the reaction proceeds conformally over all surfaces provided that the temperature is uniform. The presence of excess H_2 during the deposition effectively suppresses Cu oxidation by trace oxygen and moisture in the compressed fluid. By contrast, attempts to deposit Cu by the thermal disproportionation of Cu(I) precursors in supercritical carbon dioxide in the absence of H_2 or other reducing agents yields copper oxides.[57] Alcohols can also be used to reduce Cu(II) precursors, as demonstrated by several groups.[36,58]

One challenge for the use of reactive depositions such as CVD, ALD, and SFD in interconnect structures has been

Table 4. Summary of Metal Films Deposited by Supercritial Fluid Deposition and Their Deposition Conditions

film	precursor	solvent	reactant	deposition temp (°C)	substrate	ref
Ag	Ag(hfac)(cod)	CO_2	acetone	150−250	Ru, TaN, TiN	50
Au	(acac)Au(me)$_2$	CO_2	H_2	60−125	SiO_2, Ni, Ni−Pd−polyimide, Pd−Polyimide, Pt−Polyimide, Pd−Si, TiN	39, 41
CdS	Cd[S$_2$CN(C$_6$H$_{13}$)$_2$]$_2$.	CO_2	C_4H_9SH	315−450	SiO_2	81
Co	CoCp$_2$	CO_2	H_2	285−320	Si, TaN, TiN	38
Cu	Cu(tmhd)$_2$	CO_2	EtOH	270−300	Co, TaN, TiN, Ni, SiO_2	36
	Cu(tmhd)$_2$	CO_2	H_2	300	TaN	36
	Cu(tmhd)$_2$	CO_2	1-BuOH, 2-BuOH, MeOH, 1-PrOH,	270	Co	36
	Cu(hfac)$_2$	CO_2	H_2	180−400	TiN, Ru, Si, Au, TiN, TaN, WN	29, 43, 34, 46
	Cu(dibm)$_2$	CO_2	H_2	200−280	TiN, TaN	43, 47
	Cu(tmod)$_2$	CO_2	H_2	220−270	TiN	35
Ni	NiCp$_2$	CO_2	H_2	130−200	Si, TaN, TiN, CNT	29, 38, 48
Pd	Pd(hfac)$_2$	CO_2	H_2	60−80	polyimide, TiW, Al_2O_3	37, 45
	(π^3-C$_3$H$_5$)Pd(acac)	CO_2	H_2, thermal	40−60	polyimide, Al_2O_3	37, 45
	CpPd(π^3-C$_4$H$_7$)	CO_2	H_2	60	polyimide, Si, Al_2O_3	37, 39, 45
Pt	(cod)Pt(me)$_2$	CO_2	H_2	60−80	Si, PTFE, polyimide, Al_2O_3, mesoporous SiO_2	39, 40, 49
Rh	(acac)Rh(1,5-cod)	CO_2	H_2	60	Pd−polyimide	39
Ru	Ru(Cp)2	CO_2	H_2	250−350	Si, Au, TiN	33, 42
	[Ru(CO)$_2$Cp]$_2$	CO_2	H_2	225−300	Si	42
	Ru$_3$(CO)$_{12}$	CO_2	H_2	175−300	Si, Ta	42
	Ru(tmhd)$_3$	CO_2	H_2	175−250	Si	42
	Ru(tmhd)$_2$(cod)	CO_2	H_2	200−300	Si, Ta	42
		CO_2	H_2			

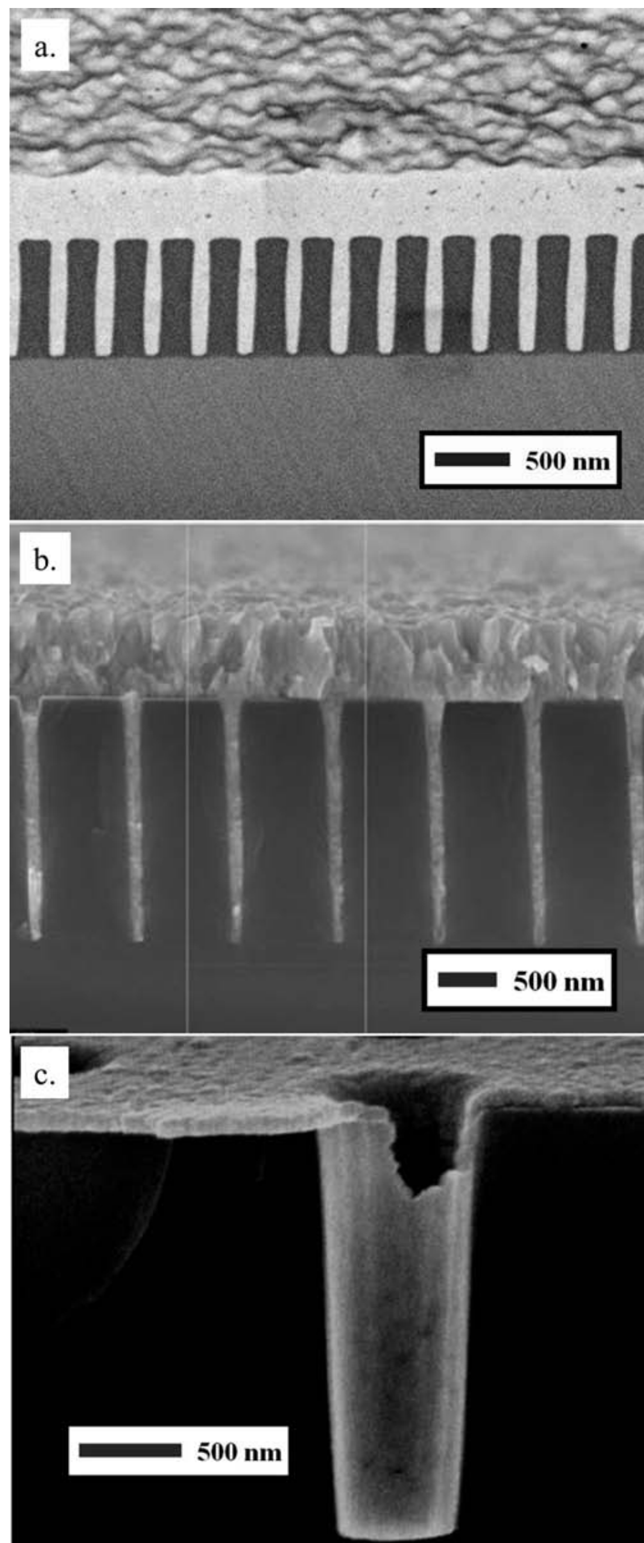

Figure 4. Metal deposition in supercritical carbon dioxide. (a) Cu deposited within high-aspect-ratio trench structures by the hydrogen reduction of hexafluoroacetylacetonate 2-butyne copper (Cu(I)(hfac)(2-butyne)).[29] (b) Conformal Ru film deposited within a trench structure by the H_2 reduction of ruthenocene in supercritical carbon dioxide.[43] (c) Conformal Ru film deposited within a via structure by the H_2 reduction of bis(2,2,6,6-tetramethyl heptane-3,5-dionato)(1,5-cyclooctadiene) ruthenium (Ru(tmhd)$_2$(cod).[42] Reprinted with permission from: (a) ref 29, Copyright 2001 American Association for the Advancement of Science; (b) ref 43, Copyright 2004 Japan Society of Applied Physics; (c) ref 42, Copyright 2006 American Chemical Society.

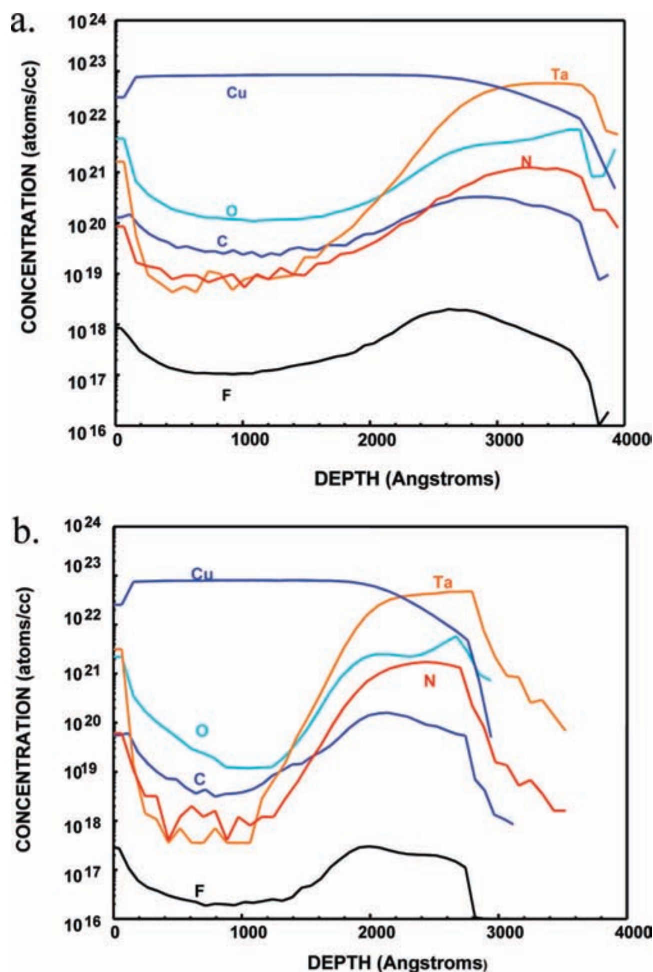

Figure 5. SIMS data for copper films deposited by (a) ethanol-assisted SFD using 0.44 wt % solution of Cu(tmhd)$_2$ in CO_2; (b) H_2-assisted SFD using 0.56% solution of Cu(tmhd)$_2$ in CO_2 at 300 °C onTaN substrates.[36] Reprinted with permission from ref 36. Copyright 2003 American Chemical Society.

the lack of adequate adhesion to adjacent barrier layers. Poor adhesion can result from oxidation of the barrier layer or contamination of the interface with decomposition products from the Cu precursors. Recently, Zong reported that the adhesion of Cu deposited by SFD to Ta, TaN, and TiN barrier layers could be dramatically enhanced by the use of sacrificial adhesion layers during the deposition.[59] The approach involves the use of ultrathin layers of poly(acrylic acid) (PAA) prepared on barrier surfaces via spin-coating or through the simple vapor phase exposure of the substrate to acrylic acid prior to metallization. Following deposition at 250 °C, no trace of the adhesion layer remains at the substrate metal interface, indicating that it was sacrificial at the deposition conditions used. Moreover, the presence and subsequent decomposition of the PAA layer during deposition substantially reduced or eliminated metal oxides at the substrate interface. On PAA-treated Ta substrates, XPS analysis indicated Ta was present primarily as Ta at the metalized interface, whereas Ta_2O_5 dominated the interface of samples prepared without the adhesion layer. The technique can be extended to patterned substrates using adsorption of acrylic acid or thermal/UV polymerization of acrylic acid. More recent quantitative analysis by Karanikas et al. using a four-point bend test indicates that the average interfacial adhesion energy when using the sacrificial PAA

surface pretreatment is just above 5 J/m^2, which meets adhesion requirements for integration in Cu interconnects.[60]

While the ability to deposit Cu directly on diffusion barriers without the need for a seed layer provides a direct single-step fill, there has been some interest in depositing thin Cu films as seed layers for subsequent electrochemical plating. Momose et al. studied the initial nucleation and coalescence of Cu films during SFD by measuring the surface reflectivity of visible white light. They found a continuous 10 nm thick film, suitable for a seed layer for electrochemical plating, could be prepared using $Cu(tmhd)_2$ at high hydrogen concentrations.[61]

Given the relatively large body of work on Cu SFD, it is informative to compare its potential against the current dual damascene process used for interconnect fabrication, which involves the deposition of a continuous, conductive Cu seed layer by physical vapor deposition (PVD) followed by a bottom-up feature fill by electrochemical plating. The step coverage of SCF processes for Cu deposition approaches 100%,[29] while step coverages of PVD processes to produce Cu seed layers are often in the range of 10−20%.[62] Poor sidewall coverage is a serious issue for continued scaling of the current dual damascene approach as continuous, conductive seed layers are required to enable feature fill by electrochemical plating. To remediate poor step coverage by PVD, corrective steps such as Cu resputter are employed. As interconnect dimensions decrease, solutions for step coverage remediation and seed layer repair become progressively more difficult. In fact, these challenges prompted significant research into process alternatives, including SFD. As noted above, the SFD process eliminates the need for the seed layer altogether and single-step gap fill of very small features can be readily achieved. Thus one advantage of the SCF process is a reduction in the number of process steps. We further note that Cu deposition rates in SFD (30 nm/min) are more than adequate for commercialization in Cu interconnect technology. At these rates, 90 nm lines and interconnects can be completely filled in under 2 min (Note the films grow from opposing surfaces, so in a trench the fill rate is twice the deposition rate). Moreover, this approach is likely extendable to end of the roadmap dimensions. Because Cu deposition is strictly conformal, aspect ratios increase rapidly and feature width decreases as the Cu films grown from opposing surfaces approach. As the films approach and impinge, an in situ annealing leads to grain growth and elimination of the seam.

One initial area of concern for SFD had been adhesion of the deposited Cu film to barrier layers relative to the excellent adhesion of films deposited by PVD. Similar difficulties had been noted for Cu CVD, where adhesion was further compromised by the use of fluorinated precursors. In fact, poor adhesion of CVD Cu films combined with difficulties in achieving acceptable step coverage at reasonable deposition rates due to low vapor phase precursor concentrations precluded further development of Cu CVD for interconnect fabrication. The use of nonfluorinated precursors in Cu SFD improved the situation markedly. Moreover, as noted above, sacrificial adhesion promoters can be used to meet industry adhesion standards for Cu films deposited by SFD.

While it is unlikely that Cu SFD would be used to produce seed layers for sub-100 nm device structures, the situation is different for large Cu structures such as through-chip interconnects for chip stacking. SFD depositions rates are well below deposition rates for electrolytic plating. In these applications, SFD fill would be prohibitively slow relative to plating, but deposition of a thin conformal film in these high-aspect-ratio features would be ideal for the plating seed layer.

Thin ruthenium films are of interest for use as both barriers and capacitor electrodes and can also be deposited with exceptional step coverage using SFD. For example, Kondoh demonstrated defect-free filling of high-aspect-ratio 100 nm wide features on seeded Si wafers by the hydrogen reduction of ruthenocene (Figure 4b).[43] We have deposited continuous and conformal films as thin as 20 nm directly within high-aspect-ratio via structures by hydrogen reduction using chemistry that does not require a seed layer.[42] Interestingly, H_2 reductions of Ru precursors proceed readily in CO_2 to yield high-purity films. This is typically not the case in CVD, where deposition under oxidizing conditions is more common and can lead to oxygen and carbon contamination that is deleterious to device performance. Recent studies confirm that high precursor concentrations during Ru SFD yield deposition kinetics that are zero order with respect to precursor concentration.[33]

There are numerous reports of the deposition of other metals including Ag, Au, Co, Ir, Ni, Pd, Pt, and Rh. Cabanas et al. have demonstrated the preparation of patterned metal films templated by an underlying substrate.[41] Gold was deposited within high-aspect-ratio vias that were etched in Si and backfilled with a thin layer of SiO_2. The gold film was then released from the substrate by etching the underlying oxide with hydrofluoric acid, yielding an array of high-aspect-ratio gold posts. Zhao et al., recently demonstrated the deposition of Ag on Ru substrates using acetone as the reducing agent.[50]

Work has also been carried out using the codeposition of multiple precursors to form films containing a mixture of materials.[63,64] For example, phosphorus-doped cobalt films (Co(P)) can be prepared by the reduction of 2,2,6,6-tetramethyl-3,5-heptanedionato cobalt in the presence of triphenylphosphine, and Pt/Ni alloyed films of tailored composition can be produced by coreduction of dimethylcylococtadiene platinum and nickelocene with H_2 in CO_2.[30,63] By operating at temperatures from 275 to 325 °C, the Co(P) films could be deposited on Cu lines selectively over the surrounding dielectric, providing an efficient means of Cu line capping.[63] In a variant of the alloy strategies, the deposition temperature of Cu and Ni films can be significantly reduced by the reduction of their precursors in the presence of trace quantities of easily reducible Pt or Pd compounds.[29,30,64,65]

Alternative metal deposition strategies have also been developed. Ye et al. deposited Cu, Ag, and Pd onto Si and Ge using HF as a reacting agent to facilitate deposition on Si and Ge surfaces.[66] The fluorination of semiconductor surfaces initiates reduction of the precursor to yield conformal metal films. Kim et al., deposited Cu films using a novel process in which Cu precursors including $Cu(hfac)_2$ hydrate films are deposited on substrates using a displacement from two immiscible supercritical phases (DISP) technique followed by reducing the copper(II) compound films in hydrogen at 200 °C.[67] The technique yielded smooth Cu films on the native oxide of Si, low *k* dielectrics, and barrier layers such as TiN.

While much of the initial work on SFD was directed toward metals, the deposition of conformal metal oxide films is important for capacitors and high *k* device layers as well

as applications in ferroelectrics,[68] membranes,[69] catalyst supports,[70] thermoelectrics,[71] and superconductors.[72] Using supercritical fluid transport and chemical deposition (SFT-CD), Hansen et al. created aerosols that were sprayed onto a heated target substrate and pyrolized at ambient pressure to yield metal oxide and mixed oxide systems, including complex superconducting oxides.[27] More recently, Uchida et al. demonstrated direct growth of TiO_2 films by spraying supercritical precursor solution directly onto a substrate heated to 80−120 °C.[73] Using reactive depositions in the presence of supercritical fluids, Gougousi et al. demonstrated that a suitable oxidizing agent, such as hydrogen peroxide or *t*-butyl peracetate, enabled low temperature deposition of planar Al_2O_3, ZrO_2, MnO_x, and RuO_x films in carbon dioxide.[74] Yttrium oxide films could be deposited by the reaction of Tris(2,2,6,6-tetramethyl-3,5-heptanedionato) yttrium(III) with hydrogen peroxide or organic peroxides in CO_2 at 130 °C.[75] Parsons investigated the thermal decomposition of metal diketonates in supercritical carbon dioxide to yield Al_2O_3, Ga_2O_3 and other metal oxides.[76] The depositions were initiated at temperatures more than 100 °C below those required in similar vacuum-based processes. A kinetic study indicated that lower activation energies and enhanced thermal decomposition rates in CO_2 are possible due to solvation of the reactant transition states. O'Neil and Watkins demonstrated an extension of the surface-selective, cold wall, SFD deposition process to yield high quality, conformal, metal oxide films at relatively low temperatures. In that work, cerium, hafnium, titanium, niobium, tantalum, zirconium, and bismuth oxide films were deposited at temperatures between 100 and 350 °C using CO_2-soluble precursors by reaction of the precursor with water present in the CO_2, either added in controlled amounts or present as an impurity in the system (see Figure 6).[77] The as-deposited films were amorphous but could be crystallized upon a high temperature annealing step. Very recently, Lee and co-workers reported the supercritical fluid deposition of $SrTiO_3$. Compared to CVD $SrTiO_3$, the $SrTiO_3$ deposited by this approach showed excellent conformality and compositional uniformity inside nanoscale features.[78] Table 5 summarizes the SFD deposition of metal oxide films and their reaction conditions.

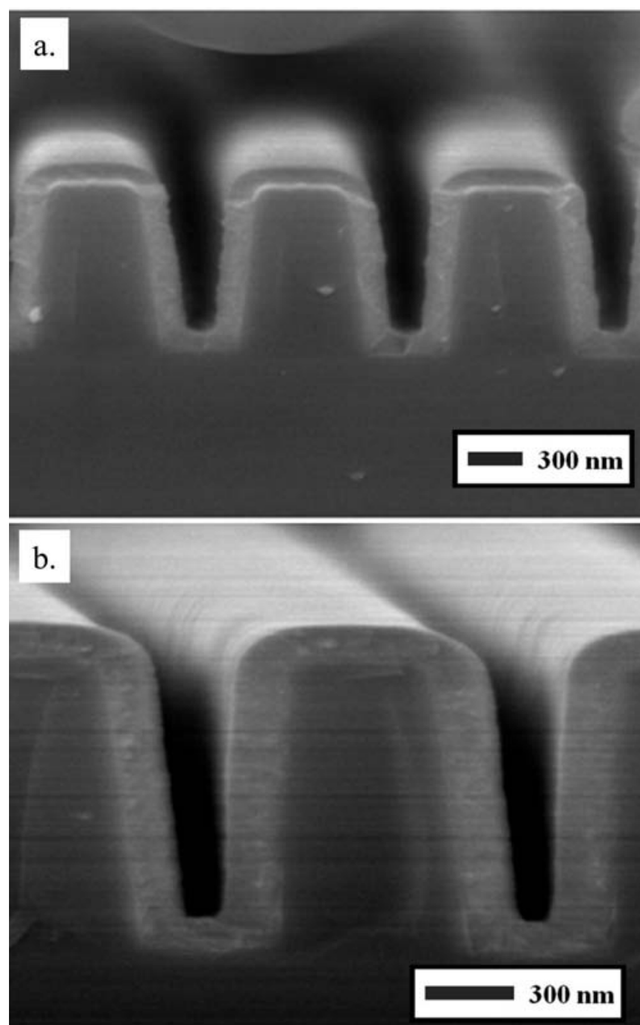

Figure 6. SEM images of films deposited on silicon nitride trench structures. (a) Hafnium dioxide deposited by hydrolysis of tetrakis(2,2,6,6-tetramethyl-3,5-heptanedionato) hafnium (Hf(tmhd)$_4$).[77] (b) Cerium oxide deposited by hydrolysis of tetrakis(2,2,6,6-tetramethyl-3,5-heptanedionato) cerium (Ce(tmhd)$_4$).[77] Reprinted with permission from ref 77. Copyright 2007 American Chemical Society.

Tsai and co-workers have demonstrated that the dielectric properties of SiO_x and HfO_2 films prepared by conventional techniques can be improved by postdeposition treatment with supercritical CO_2.[79,80] Treatment of SiO_x films prepared by electron-gun evaporation with supercritical CO_2 solutions of ethyl alcohol and H_2O increases the oxygen content of the SiO_x films and terminated traps within SiO_x by forming Si−O−Si bonds, leading to reductions in leakage current. Exposure of ultrathin HfO_2 films deposited on p-type (100) Si wafer by DC sputtering to supercritical CO_2 at 150 °C likewise increased oxygen content, reduced traps in the HfO_2 films, and decreased the equivalent oxide thickness.

Recently, SFD has been extended to the deposition of semiconductors. Smith and co-workers recently demonstrated the deposition of optoelectronic quality CdS thin films in a series of supercritical CO_2 continuous flow reactors from the single source precursor, $Cd[S_2CN(C_6H_{13})_2]_2$.[81]

The work of numerous groups summarized in the preceding discussion indicates that SFD provides a viable and in certain cases enabling route to the reactive deposition of metal, metal oxide, and most recently semiconductor films for nanoscale device fabrication. The advantages of the technique include single-step conformal coverage, high precursor utilization, and high film purity. From a cost of ownership point of view, we expect SFD to be similar to CVD. Both are single-wafer batch processes that require pressure sealing. While the high pressure requirements of SFD may be slightly more costly than a vacuum process, the comparatively high utilization of precursors for SFD relative to CVD should provide adequate offset. On the basis of film growth rates, residence times and throughput would be similar for the two techniques.

While a broad range of materials have been deposited successfully by SFD, virtually all deposition chemistries rely on those developed for CVD, where volatility is a primary design constraint. One important area for future development is the design of precursors tailored specifically to SFD. Removal of the volatility constraint should enable new chemistries. For example, thermal stability requirements of potential SFD precursors can be less than those of CVD precursors, which are often delivered at elevated temperatures. This in turn provides pathways for film deposition at low temperature and on thermally labile substrates.

The extension of SFD to CdS is a promising indictor of the potential of this technology for the deposition of device

Table 5. Summary of Metal Oxide Films Deposited by Supercritial Fluid Deposition and Their Deposition Conditions

film	precursor	solvent	reactant	deposition temp (°C)	substrate	ref
Al_2O_3	$Al(acac)_3$	CO_2	H_2O_2, *t*-butyl peracetate, H_2O, O_2	70−250	Si	74, 76
	$Al(hfac)_3$	CO_2	H_2O_2, *t*-butyl peracetate	80−150	Si	74
BiO_x	$Bi(Ph)_3$	CO_2	H_2O	350	Si	77
CeO_x	$Ce(tmhd)_4$	CO_2	H_2O	250	Si	77
Ga_2O_3	$Ga(acac)_3$	CO_2	H_2O, O_2	160−250	Si	76
HfO_2	$Hf(tmhd)_4$	CO_2	H_2O	300	Si	77
MnO_x	$Mn(hfac)_2$	CO_2	H_2O_2	100−150	Si	74
NbO_x	$Nb(tmhd)_4$	CO_2	H_2O	300	Si	77
RuO_x	$Ru(tmhd)_3$		H_2O_2, *t*-butyl peracetate	100−150	Si	74
$SrTiO_3$	$Sr(tmhd)_2$ and $Ti(mpd)(tmhd)_2$	CO_2	H_2O_2	75−380	Si	78
TaO_x	$Ta(OEt)_4(acac)$	CO_2	H_2O	300	Si	77
TiO_2	$Ti(tmhd)_2(iOPr)_2$	CO_2	H_2O	300	Si	77
Y_2O_3	$Y(tmhd)_3$	CO_2	H_2O_2, *t*-butyl peroxide, *t*-amyl peroxide	80−150	Si	74, 75
ZrO_2	$Zr(acac)_4$	CO_2	H_2O_2, *t*-butyl peracetate	120−200	Si	74
	$Zr(tmhd)_4$	CO_2	H_2O	300	Si	77

quality semiconductor films, and further work in that direction is certainly warranted. Another fertile area for development is the deposition of alloys and doped metal and metal oxide films wherein precursors for the desired materials can be mixed at desired compositions according to their solubility limits without balancing vapor pressures. There are some examples in the patent and journal literature, but many potential avenues remain. There has also been little work on depositions that employ the oxidation of precursors despite that fact that CO_2 is oxidatively stable and provides an excellent medium for such chemistry.[16,82,83] When considering deposition candidates for SFD, limitations also apply. The high fluid density results in a relatively high concentration of trace gases such as O_2 and water that can be problematic for oxophilic metals. In cases such as Cu where oxidation can be completely suppressed by the use of a reducing environment (e.g., hydrogen assisted depositions) this is not an issue, but for many metals it is a limitation.

The results from deposition studies using cold wall reactor configurations using 2" wafers do not indicate obvious issues of concern with respect to scalability for Cu and other metals. However, unlike the cases of cleaning and ULK film preparation in CO_2, a full 200 or 300 mm wafer tool for depositions has not yet been built and validated. The construction of such a tool is required for moving forward. Such an effort will require a better understanding of reactor fluid mechanics, as turbulent flow in SFD reactors driven by the thermal gradients in the compressed fluid is a significant departure from laminar flow CVD reactors. Studies by computational fluid dynamics indicate sufficient clearance between the stage and reactor ceiling to permit the development of recirculating flow is required to maintain uniform temperature profiles across the wafer. Ignoring this fact leads to nonuniform films.[56] Commercialization will also require CO_2 purification, the development of tool cleaning protocols, and possibly particulate management strategies. One of the major barriers to implementation of Cu deposition by SFD for interconnect structures, adhesion to the barrier layer, has been resolved at the laboratory scale and shown to meet integration requirements.[59,60] The next step requires the fabrication of test structures for yield and failure analysis.

3.2. Metal and Metal Oxide Etching in Supercritical Fluids

Device fabrication often requires the removal of metals and metal oxides by etching for contamination control and for pattern generation. Dry etching is often limited by either the volatility of the etching agents or resulting metal chelate or halide byproduct. For example, anisotropic Cu metal etching can be limited by the volatility of Cu halides.[84] As with SCF deposition processes, a supercritical fluid can be used to overcome species volatility constraints for dry etching.[84−90] DeSimone and co-workers demonstrated the etching of Cu in supercritical carbon dioxide using solutions of organic peroxides and hexafluoroacetylacetone (hfacH) free ligand.[86] Using their approach, the peroxides are necessary to oxidize the copper. The oxides can then be etched using hfacH as the chelating agent, resulting in removal of the metal film. Muscat and co-workers conducted a detailed study of the etching of copper by sequential oxidation at ambient conditions followed by exposure to (hfacH) in supercritical CO_2.[84] A kinetic model and mechanism were later developed for the heterogeneous chelation reaction of thin CuO films with hexafluoroacetylacetone (hfacH) in supercritical CO_2. A maximum etching rate of approximately 2.5 nm/min was observed over a temperature range of 54−88 °C. The kinetic studies indicated an apparent activation energy of 70.2 ± 4.1 kJ/mol and an order of approximately 0.6 with respect to hfacH.[90] Shan and Watkins studied the etching kinetics of cuprous oxide films (Cu_2O) supported on Cu or on SiO_2 using several β-diketones including (hfacH), 2,2,6,6-tetramethyl-3, 5-heptanedione (tmhdH), and 2,2,7-trimethyloctane-3, 5-dione (tmodH) in supercritical CO_2 at temperatures between 80 and 150 °C and pressures between 200 and 275 bar.[88] At 150 °C, the etch rate using tmodH was 1.5 nm/min. On the basis of the activation energy obtained from the studies (65 kJ/mol), etch rates greater than 10 nm/min can be obtained at 200 °C. Carrying out the etching chemistry in supercritical CO_2 enables the use of nonfluorinated chelating agents such as tmhdH and tmodH, which reduces fluorine contamination in the films and lessens environmental, health, and safety concerns.

Irene, DeSimone and co-workers studied the etching of silicon dioxide films grown on single crystal Si using nonaqueous HF and HF/pyridine solutions in supercritical CO_2.[91,92] Etch rates of several nm/min were reported for HF/pyridine solutions in CO_2 at temperatures between 35 and 55 °C. Post-etch SiO_2 regrowth and testing indicated that Si surfaces produced via the SCF process are electronically comparable to those produced using conventional techniques.[92]

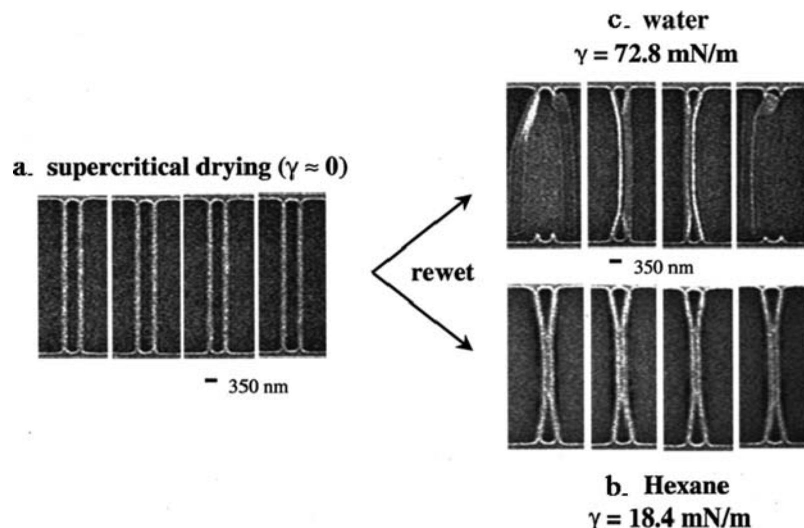

Figure 7. Top-down SEM image of APEX-E photo resist that were dried in (a) supercritical CO_2, (b) hexane, and (c) water.[93] Reprinted with permission from ref 93. Copyright 2007 American Institute of Physics.

While work by several groups indicates that metal and metal oxide etching are possible in supercritical CO_2, the path to commercial adaptation is not clear. For dry etch processes in which the volatility of the etching agent or the resulting metal complex is limited, the use of a supercritical fluid offers potential benefits. The literature to date, however, has not indicated that such strategies offer new capabilities rather than an alternative method that achieves a similar result. The same is true of comparisons of SCF processes to wet etching in which the motivation for some of the work has been to replace or conserve water rather than provide new capability. Future work should clearly identify a differentiating technical advantage.

3.3. Photoresist Processing and Development

The combination of liquid-like densities with the absence of surface tension has generated much interest in the use of supercritical fluids for drying of nanoscale features and for the processing and development of photoresists. Supercritical drying has been widely applied to nanostructured materials and devices including aerogels and microelectromechanical systems to avoid damage that can occur by capillary forces during the removal of liquid solvents. The field is well reviewed elsewhere[4,7,12,93,94] and will not be discussed in detail here beyond few examples relevant to device manufacturing. Goldfarb et al. used a CO_2/hexane/surfactant system to dry high-aspect-ratio resist patterns without feature collapse.[93,95] The resist lines were 140 nm thick, with a spacing of 370 nm and an aspect ratio of 6.8. Conventional drying of these structures when rewetted with water and hexane led to structural collapse (Figure 7). Namatsu et al. demonstrated solvent removal from 7 nm resist features with an aspect ratio of 10, also using a surfactant, and recently used water displacement with SF_6 followed by supercritical removal to effectively dry surfaces without damage.[94,96,97] Lee and co-workers examined the efficacy of a series of hydrocarbon, fluorocarbon, and polymeric surfactants in CO_2 to remove water from aqueous-based resist systems.[98]

CO_2 has also been used for both spin-coating[3] and the direct development of polymer-based and molecular glass photoresists. The most successful demonstrations have been those which have employed components that are readily soluble in supercritical carbon dioxide. These include fluorinated acrylates or silicone-based polymers and some molecular glass species. These studies differ from attempts to strip conventional photoresists, which typically exhibit very poor or no solubility in supercritical carbon dioxide, from device structures and are discussed later.

Ober et al. demonstrated the direct development of negative-tone resists comprised of copolymers of tetrahydropyranyl methacrylate and fluorinated methacrylates. Acid cleavage of exposed tetrahydropyranyl groups rendered a solubility difference sufficient for CO_2 development.[99] This system was later modified to provide a high-resolution positive-tone resist that could be developed in CO_2.[100] Resist systems for CO_2 development have also been reported by DeSimone's group.[101] More recently, Ober's group reported the first intrinsically positive-tone resist system that is developable in supercritical CO_2.[102] The system is based on acid-catalyzed depolymerization of an acetal-based polymer such that the decomposition products are appreciably more soluble in supercritical CO_2 than the base polymer. Because the system involves the dissolution of the small molecule acetal polymer decomposition products rather than a polymer, fluorinated or silicone groups are not required to induce solubility.

Molecular glasses (MGs) have received much recent attention as next generation resists, in part due to their high glass transition temperatures, good thermal stability, capacity to form high quality amorphous films, and their relatively small molecular dimensions relative to polymeric resists, which could lead to reduced line edge roughness. Moreover peripheral hydroxyl and carboxylic acid functionality that decorate the molecular glass cores can be protected and deprotected using chemistry similar to that employed in chemically amplified resists. Deprotection of the molecular glass upon exposure to UV light in the presence of a photoacid generator thus provides a means to induce a polarity switch for development. In the case of a supercritical CO_2-based medium, the protected MG is soluble in the fluid, whereas the deprotected MG is much less soluble. Shiraishi and co-workers reported the solubility of several protected and deprotected polyphenols in CO_2 to demonstrate the development concept.[103] Ober demonstrated high resolution patterning using CO_2-developable MG resists including calix[4]resorcinarene derivatives.[104,105] The structure of sev-

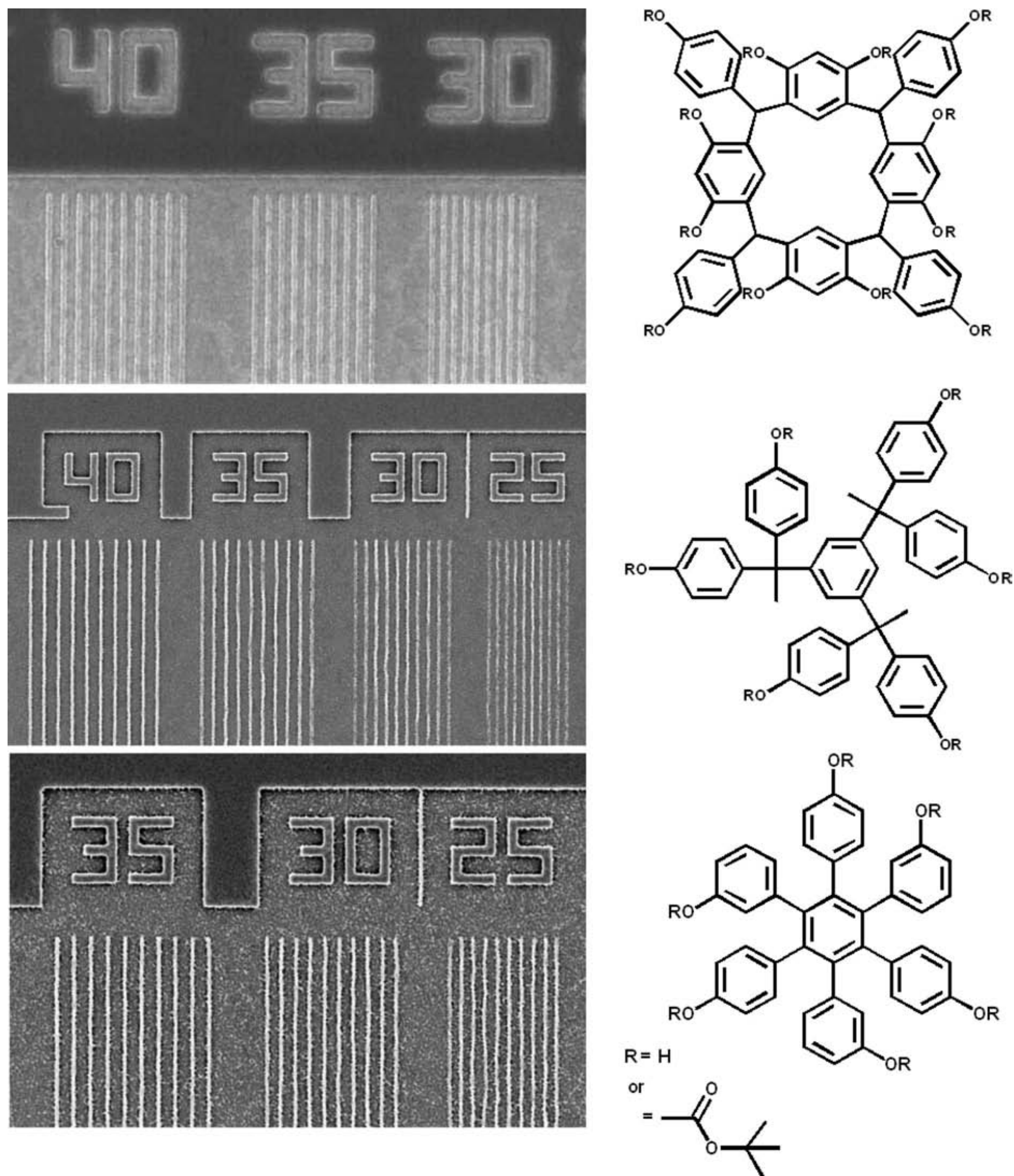

Figure 8. High resolution EUV patterning using three different molecular glasses, developed in CO_2.[104] Reprinted with permission from ref 104. Copyright 2008 Wiley-VCH.

eral resists and images of the films following e-beam patterning and CO_2 development are shown in Figure 8.

Development of conventional resist platforms in supercritical CO_2 is difficult due to the poor solubility of styrenic and nonfluorinated acrylate polymers in carbon dioxide. The development of a practical strategy for the development of standard resists, rather than processes that rely on new materials, could improve the potential for adaptation. Recently, Wagner et al.[106,107] reported the direct negative tone development of extreme-ultraviolet (EUV) resists in homogeneous carbon dioxide solutions containing CO_2-compatible salts (CCS) that are positive tone under aqueous development. The additives, which are essentially quaternary ammonium salts, are selected such that the anion or the cation contains at least one CO_2-soluble portion. Complexation of the salt with the deprotected resist provides a means for dissolving the polymer and affecting development. These results have led to additional studies to elucidate the mechanisms for development, optimize development conditions, and demonstrate efficacy for a variety of resist platforms.[108−110] Figure 9 show a schematic of the process and a comparison to conventional tetramethylammonium hydroxide (TMAH) development.

In Wagner's work, standard positive tone EUV resists were developed in supercritical CO_2 containing less than 20 mM CCS at pressures ranging from 240 to 380 bar, 35 to 65 °C with cycle times as short as 1 min to give reverse image development. Substantial reduction in image collapse and

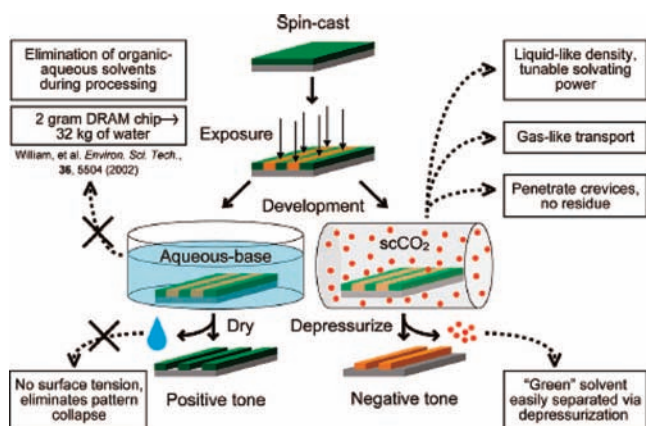

Figure 9. Comparison between conventional aqueous-base and $scCO_2$ processing.[108] Reprinted with permission from ref 108. Copyright 2009 American Chemical Society.

line edge roughness was observed. Aspect ratios approaching 10 were possible in dense line/space features, and dense lines with 3σ line width roughness values that are 30% smaller than comparable TMAH-developed samples were obtained.[106] A comparison of features developed using aqueous TMAH and CO_2 solutions is shown in Figure 10. Because EUV resists can be structurally similar to 248 nm resist platforms, the technique has the potential for broad applicability.

Recent studies provide additional insight into the CCS development strategies in supercritical CO_2. Carbonell, Wagner, and co-workers studied the absorption of CO_2 and CCS candidates into photoresists at conditions relevant to development using a quartz crystal microbalance.[109] The same group recently reported cloud point measurements for EUV resists in CO_2/CCS solutions and the kinetics of resist dissolution. Pressures on the order of 200 bar are sufficient to dissolve the resist systems. Dissolution kinetics indicate that development times are on the order of a few minutes. Contrast curves for the EUV resists were generated to determine the sensitivity of the resists and development contrast using standard TMAH solutions and CCS solutions in CO_2. TMAH provides positive tone development while, as expected, the tone is reversed using CCS in CO_2. At the conditions studied, the CCS route showed improved sensitivity and better contrast relative to TMAH development, which is quite encouraging.[110] Ober and co-workers studied CCS assisted development resists following 248 nm or e-beam lithography using a series of fluorinated CCS materials in CO_2 and compared the results to development in TMAH. Contrast curves were sharp for some of the CCS candidates relative to TMAH and showed tone reversal for the CCS route (negative tone) relative to TMAH (positive tone). Resist removal rates on the order of 15−40 nm/min for EUV (a TOK commercial resist) and 248 nm (poly(4-*t*-butoxycarbonyloxystyrene) resists using CCS in CO_2 were reported. A molecular level view and mechanism for the development was described by computer simulation.[106]

Overall, recent progress in CO_2 resist development offers promising opportunities for implementation. Both the molecular glass and CCS development schemes are designed with the solvent characteristics of CO_2 in mind and can be operated at modest pressures and relatively low solvent volumes. Simple isothermal reactors can be employed. The CCS approach is particularly attractive because it builds on existing resist platforms and does not require the qualification of new materials. Contrast curves confirm good performance relative to existing schemes. Both approaches effectively prevent pattern collapse. Further development of the systems will require demonstration of high resolution, acceptable line edge roughness for small features and means to recover and recycle the CCS salts.

3.4. Wafer Cleaning and Photoresist Stripping

Wafer cleaning and photoresist stripping are among the areas of SCF technology that received the most attention for applications development for the semiconductor industry. In principle, the attributes of supercritical fluids, including carbon dioxide, offer advantages to traditional media. These include the absence of surface tension, which prevents pattern collapse in lithographically defined features and allows access to nanoscale pores in ultralow *k* dielectrics and the enablement of an all dry process because CO_2 is a gas at room temperature and pressure. The environmental benefits of using CO_2 as a process solvent have also been discussed. Specific applications, including photoresist stripping and cleaning, cleaning of post etch and post ash residues, metal ion removal, and particle removal are reviewed extensively elsewhere and will not be discussed beyond a brief summary in this article.

A significant challenge for the use of carbon dioxide as a medium for cleaning and stripping is that CO_2 is a weak solvent for the materials to be removed, including ionic, particulate, and metallic species as well as most polymers. Consequently, appropriate additives packages are necessary. These include polar cosolvents, chelating agents, and surfactants. The latter can be engineered to form reverse micelles or microemulsions in CO_2 such that polar domains containing water are dispersed in the continuous CO_2 phase. Solvation of the contaminants in the polar domains permits their removal and transport from the surface. The majority of the surfactants contain fluorocarbon tails due to their CO_2-philic nature. Success with a few hydrocarbon- and silicone-based surfactants has also been reported.[4]

The situation for photoresist stripping is complicated by the very poor solubility of most photoresist polymers in CO_2. This is especially true for situations in which the resist is cross-linked during processing. The solutions again require cosolvents to improve dissolution and physical and chemical means to break up and dislodge residues. A number of tool manufacturers also designed for high operating pressures to maximize the density of CO_2. However, this approach yields marginal gains as CO_2 becomes less compressible at higher operating pressures. For insoluble resists, processes used to break up and/or delaminate the resist include pulsed flow, ultrasonic agitation, and ablation. The resulting particulates must then be removed. One notable effort in the area is the supercritical CO_2 resist remover (SCORR) cleaning system developed at Los Alamos. They demonstrated the removal of resist by using a pressure pulse (76−110 bar) of a CO_2/propylene carbonate cosolvent solution to dislodge the resist followed by a rinse containing additives such as alcohol, water, and acetone. This technology was later licensed to a commercial venture. Recent work describes the use of ultrasonic agitation in combination with supercritical CO_2 and cosolvents to strip high-dose implanted photoresist.[111]

While a number of studies have demonstrated the efficacy of CO_2 cleaning and photoresist stripping, there are several barriers to implementation. These include the need to demonstrate a compelling advantage to aqueous-based

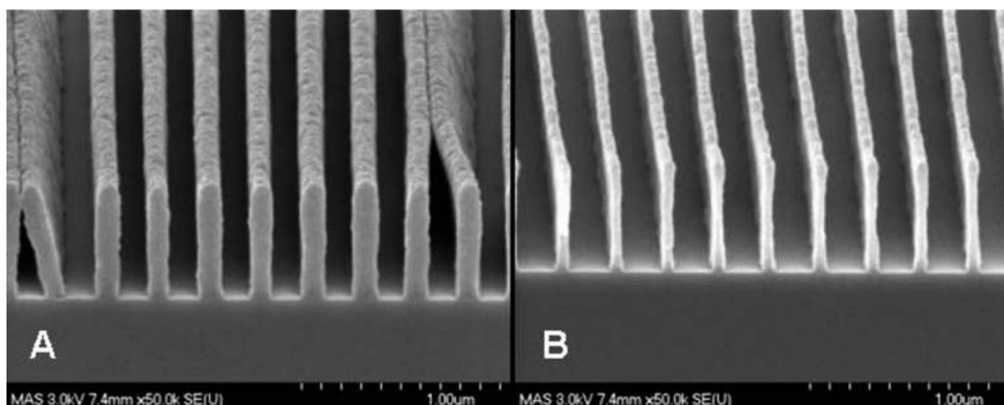

Figure 10. Cross section SEM images of a wafer patterned at 130 nm 1:1 L/S developed in: (A) aqueous TMAH and (B) with CCS chemistry in supercritical CO_2 ([A] = 10 mM, T = 60 °C, P = 345 bar, time = 1 min). The TMAH developed sample shows collapsed structures with an aspect ratio of ~4.5, while the CCS developed sample shows noncollapsed structures with an aspect ratio of ~12.8.[106] Reprinted with permission from ref 106. Copyright 2006 International Society for Optics and Photonics.

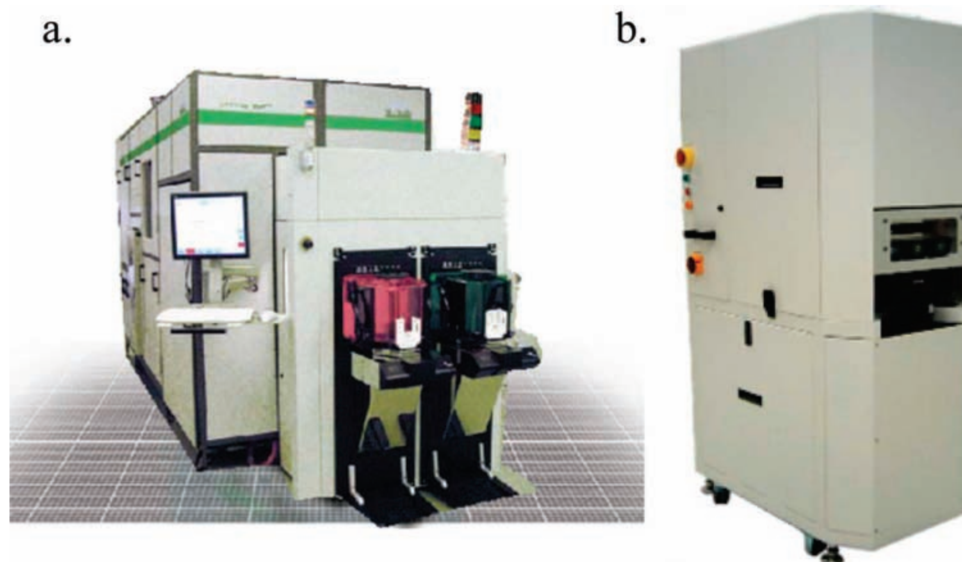

Figure 11. Commercial tooling for supercritical CO_2 processing: (a) 300 mm wafer tool developed by SC Fluids, Inc.;[150] (b) 200 mm tool developed by BOC Edwards.[151] Reprinted with permission from: (a) ref 150, Copyright 2003 SC Fluids, Inc.; (b) ref 151, Copyright 2002 BOC Edwards.

systems that provide a technical driver for change. In addition, cleaning processes typically require the recirculation and purification of large quantities of CO_2, often tens to hundreds of times that of the process vessel volume, which can increase operating and capital costs. This differs for most deposition processes, which require low solvent volumes. Particulates are also an issue due to both the very large solvent volumes and the fact that the majority of the stripping schemes do not completely dissolve the resist but rather generate particulates during resist breakup that must be removed and excluded from recirculation. Finally, environmental advantages must be evaluated on a systems basis and include the potential impacts of the additive packages.

Despite these barriers, several companies have produced high pressure full wafer process tools on cluster platforms that could be integrated into process lines. Two examples are shown in Figure 11. While SCF cleaning has not been implemented at the fab scale to date, functional tools that solved many of the engineering challenges for the implementation of SCF technology were built, presumably supported by cost of ownership calculations that showed a competitive cost structure compared to existing, relatively inexpensive alternatives. This suggests a viable pathway for the adaptation of other processes that offer compelling technical or economic advantage. Given the history and process challenges, those applications are more likely to first emerge outside the scope of stripping and cleaning.

3.5. Ordered Porous ULK Films

One challenge facing the semiconductor industry has been the development of porous, ultralow dielectric constant (ULK) thin films for use in the lower metallization layers of next generation devices. These films must exhibit sufficient mechanical integrity to survive chemical mechanical planarization and packaging and are compatible with current integration schemes. Issues concerning integration include contamination of the porous dielectric, patterning, cleaning, and etch repair. There is substantial experimental and theoretical work that indicates porous organosilicate films with ordered spherical pores offer mechanical advantages to films with disordered pore structures.[112,113] One advantage of a well-ordered periodic structure is that concerns regarding pore coalescence that result in larger scale defects are obviated.

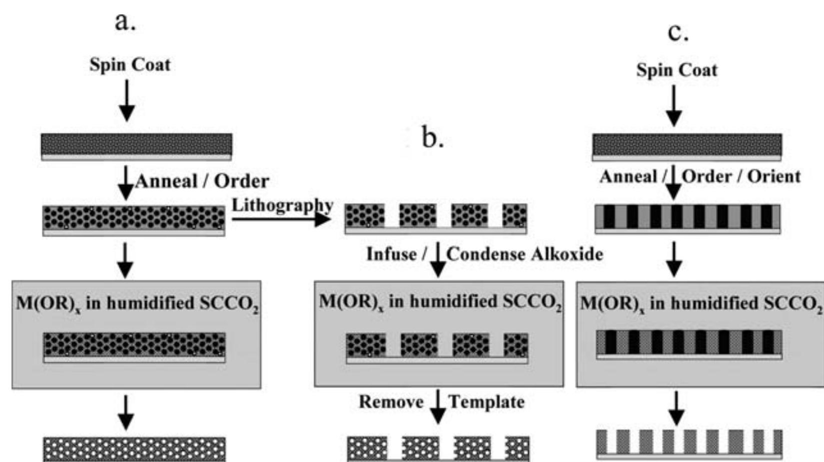

Figure 12. Schematic illustration of the process for 3D replication of block copolymer templates in supercritical CO_2: (a) template is spincoated onto a silicon wafer, (b) template is patterned by lithography, and (c) a cylindrical morphology block copolymer is aligned perpendicular to the wafer before silica infusion.[123] Reprinted with permission from ref 123. Copyright 2004 American Association for the Advancement of Science.

Practical realization of ordered mesoporous ULK films requires a facile approach that enables precise control over film composition and structure at the nanoscale. While realization of complete control of these issues for metal oxide films has proven to be very difficult, preparation of the analogous structures in polymers through self-assembly is readily at hand. We have shown that self-assembled polymer systems can serve as templates for the rapid and efficient production of robust ULKs. Specifically, the use of supercritical fluids provides a direct route for high-fidelity three-dimensional replication of these polymer templates in metal oxides including silicates. Such a route is shown schematically in Figure 12.

Block copolymers (BCPs) are nearly ideal templates for nanostructured materials. They consist of two or more polymer segments covalently bonded together and are capable of self-assembly into ordered arrays of microdomains with dimensions on the order of 5−100 nm.[114] The size, shape, and spacing of the domains can be controlled by adjusting composition (block volume fractions) and block length. Moreover, BCP films can be processed over large areas on Si wafers using processes amenable to high-volume manufacturing. Recent advances have demonstrated unprecedented opportunities for controlling domain order and orientation using controlled solvent evaporation and topological constraints.[115−118] The interaction of polymers with supercritical fluids enables the replication of polymer nanostructures by phase-selective deposition reactions within the templates. Most polymers are insoluble in CO_2 but can be swollen by fluid sorption at modest temperatures and pressures. This sorption is equilibrium-limited and can be precisely controlled (Figure 1d). Dilation of the template in supercritical CO_2 significantly enhances the mobility of polymer chains and the diffusion of small molecules within the polymer film[24,119] by depressing the glass transition temperature (T_g)[22] without disturbing the phase segregation.[120,121] Under these conditions, SCF-dilated polymer films can be good reaction media. Confinement of deposition reactions within one phase of a dilated block copolymer provides an opportunity to use these materials as templates for nanostructured films. The replication scheme shown in Figure 12 is straightforward. It involves spin-coating a suitable template onto a support, transferring the template to a high-pressure reactor for SCF-assisted infusion and deposition within the template, and removal of the template following decompression by calcination, reactive plasma, or other techniques. The key to the process is imparting selectivity for the deposition reaction during the infusion, which can be achieved by localizing a catalyst within one domain of the phase segregated polymer template. While it is possible to infuse very thin low T_g template films directly using tetraethyl orthosilicate (TEOS) vapor, the resulting silica films are typically inhomogeneous at thicknesses above a few tens of nanometers due to transport limitations and the appearance of capping layers.[122]

Figure 13 shows scanning electron micrograph cross sections of silica films prepared using this approach. In these examples, poly(ethylene oxide)-poly(propylene oxide)-poly(ethylene oxide) (PEO-*b*-PPO-*b*-PEO) triblock copolymer surfactants, known commercially as Pluronic, were used as templates and were spin-coated onto Si wafers from ethanol solutions containing *p*-toluene sulfonic acid (pTSA).[123,124] Upon solvent evaporation, the block copolymer microphase separates to yield an ordered morphology, and the pTSA segregates to the hydrophilic PEO block of the copolymer. The silica films are then prepared by exposure of the templates to solutions of TEOS or other Si alkoxides in humidified CO_2. During infusion of the template, silica condensation occurs only in the PEO domains of the template, which contains the pTSA catalyst. No condensation occurs in the SCF phase, as the catalyst is insoluble in CO_2. Following depressurization, template removal by calcination yields the silica replica.

The composition of the metal oxide films prepared by this approach can be tuned by selection of the metal alkoxides. Infusion of BCP templates with mixtures of TEOS and methyltriethoxysilane (MTES) yields robust, ordered, mesoporous organosilicate films that are exceptional candidates for use as ultralow *k* thin films for microelectronics. The mechanical and electrical properties of films containing spherical pores can be tuned by adjustments in alkoxide precursor mixtures and by adjustments in the mass uptake of silicate in the polymer templates during infusion. Defect-free, uniform films prepared on 200 mm wafers exhibiting a dielectric constant of 2.2 were metalized with copper and shown to withstand the rigors of chemical mechanical planarization, a crucial test required for device integration.[123] As feature sizes continue to decrease, pore diameters must

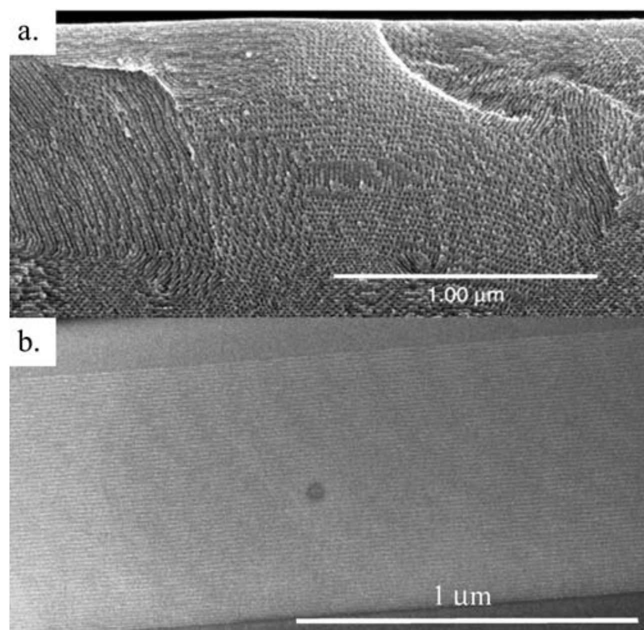

Figure 13. Nanostructured metal oxide films prepared by 3D replication of block copolymer templates in supercritical CO_2. (a) Scanning electron microscopy (SEM) image, showing cross section of ordered mesoporous silica synthesized from Pluronic F127 (PEO_{106}-*b*-PPO_{70}-*b*-PEO_{106}).[123] (b) Cross sectional SEM of highly ordered mesoporous silica synthesized from a blend of Pluronic F127 and poly(hydroxy-styrene) (16.7 wt %) template.[117] Reprinted with permission from: (a) ref 123, Copyright 2004 American Association for the Advancement of Science; (b) ref 125, Copyright 2007 American Chemical Society.

as well. Tirumala et al. demonstrated the fabrication of well-ordered mesoporous films with pores on the order of 2−3 nm by the 3-D replication of block copolymer templates blended with associating homopolymers.[125] Recently, Pai extended the scope of the 3-D replication technique by the fabrication of mesoporous silicate films using bridged silsesquioxanes including bis(triethoxysilyl)ethane, bis(triethoxysilyl)methane, and bis(triethoxysilyl)ethylene.[124] These precursors have been shown to produce robust films with good electrical properties via other techniques.[126]

A detailed study of the pore structure in the films prepared via the SCF replication technique indicated a substantial fraction of microporosity in the pore walls, which contributes to the low dielectric constant without unduly compromising film strength.[127] Recently, Vogt and co-workers showed that the pore size in the films template using blends containing Pluronic surfactants can be manipulated by controlling pressure during the infusion step. Pore sizes increased slightly (1.6−1.81 nm) as the CO_2 pressure was increased to 80 bar.[128] A small additional increase in pressure to 84 bar, slightly above the critical pressure of CO_2, resulted in a significant expansion of the pore size. The use of alternative template systems provides a means to control pore size, morphology, orientation, and long-range order.[125,129,130] Blends of poly(acrylic acid) or poly(4-hydoxystyrene) (PHS) with Pluronic F127 (PEO_{106}-*b*-PPO_{70}-*b*-PEO_{106}) or Brij 78 (poly (ethylene oxide$_{20}$-*b*-ethylene$_{18}$)] copolymers yield well-ordered cylindrical pores with center to center *d*-spacings of approximately 11 and 6 nm, respectively.[125] Transmission electron microscopy shows that F127/PHS blends in particular show exceptional long-range order (Figure 13b). Ordered arrays of cylindrical domains oriented normal to the wafer surface are also possible. Nagarajan et al. prepared

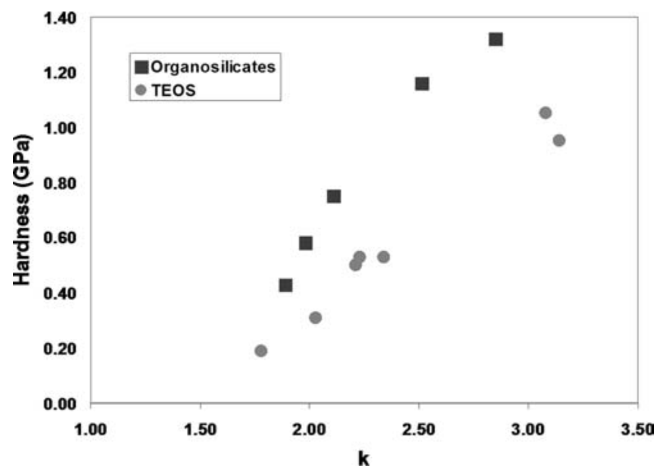

Figure 14. Dielectric constant vs hardness of mesoporous silicate films synthesized in supercritical CO_2.[123] Reprinted with permission from ref 123. Copyright 2004 American Association for the Advancement of Science.

such films by infusion of TEOS into cylindrical poly(α-methylstyrene)-*b*-poly(hydroxystyrene), PMS-*b*-PHOST copolymer templates,[131] which orient spontaneously upon spin-coating from propylene glycol methyl ether acetate.[132] The diameter of the channels can be easily adjusted by using copolymers of varying molecular weight.

It is important to point out that the low *k* films via 3-D replication can be prepared on full process wafers with good uniformity and short cycle times, which are vital for successful implementation. Moreover, this approach can be conducted in very simple, isothermal reactors with low process volumes of CO_2. The wafers can be stacked in a simple cassette to further reduce per wafer cycling times.

The electrical and mechanical properties of ULK films prepared by the SCF template replication technique compare favorably to leading candidates for integration produced by plasma enhanced chemical vapor deposition (PECVD). Figure 14 shows modulus and hardness vs dielectric constant for families of TEOS-based silica films and TEOS and methyltriethoxysilane-based organosilicate films produced by polymer template replication in supercritical CO_2 followed by calcination at 400 °C. The calcinations serve the dual purpose of removing porogen and providing a post synthesis thermal cure. For a $k = 2.2$ film, a hardness of 0.9 GPa was achieved. By comparison, leading porous SiCOH-based films produced by PECVD followed by a UV cure with $k = 2.4$ exhibit a hardness of 0.7 GPa and a modulus of 4.6 GPa while $k = 2.2$ films exhibit a modulus of 2.7 GPa.[133,134] The performance of the SCF films is especially encouraging in light of the differences in film curing, thermal for SCF vs UV for the PECVD SiCOH films. UV curing is known to approximately double the hardness and modulus of porous organosilicate films relative to thermal cures.[134,135] The data shown in Figure 14 was published prior to the adaptation of UV cures, but subsequent work in our group suggest similar trends can be realized for films produced via polymer template replication in SCFs.[136] While the ULK films produced by the SCF technique offer excellent properties, the opportunities for commercialization would be further enhanced by continuing to improve their mechanical properties and by demonstrating a lower cost of ownership for the overall process.

Other strategies for the fabrication of dielectrics using CO_2 have also been developed. Lubguban and co-workers[137,138]

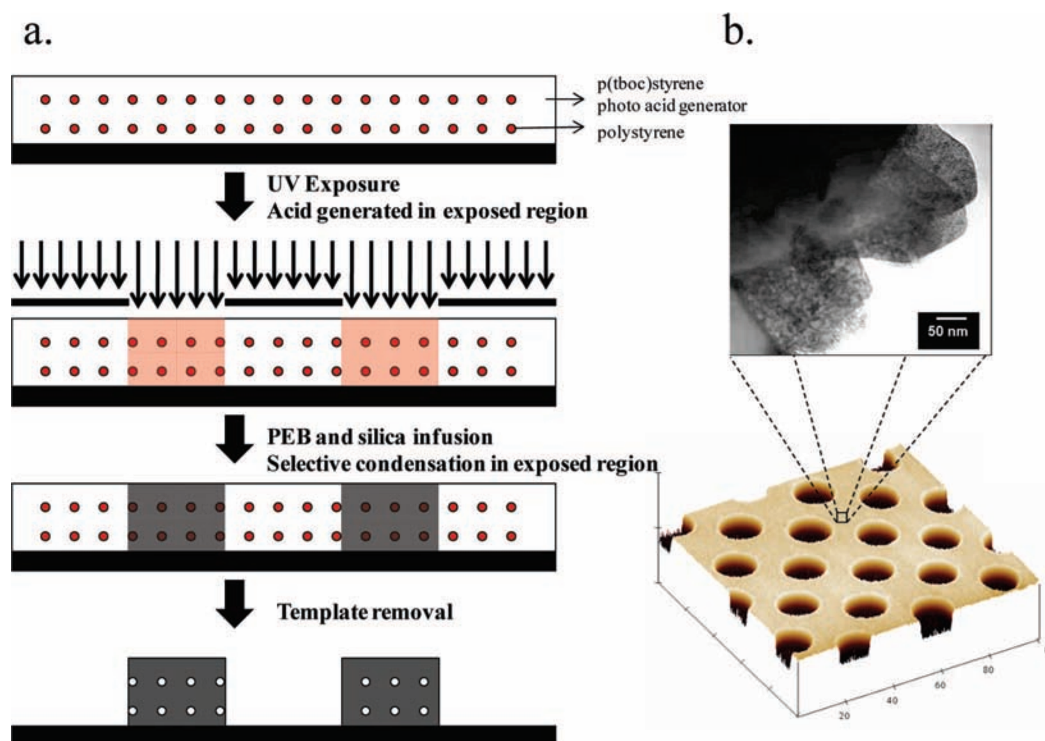

Figure 15. (a) Schematic of direct patterning process utilizing photolithography and supercritical CO_2 infusion process to produce patterned mesoporous silica without an etching step. (b) AFM and TEM images of patterned mesoporous silica synthesized through the direct patterning approach with a PS-*b*-PtbocSt block copolymer as template. The AFM image shows the device level patterning, while the TEM image shows domain level porosity arising from the block copolymer template.[130] Reprinted with permission from ref 130. Copyright 2008 American Chemical Society.

prepared ULK films by a spin-on technique using either poly(methylsilsesquioxane) as precursor for the matrix and poly(propylene glycol) as the porogen or by a cooperative self-assembly approach using surfactants as the structure directing agents and TEOS or other silicon alkoxides as the network precursor. The porogens or surfactants were then extracted from the films using mixtures of supercritical CO_2 with methyl ethyl ketone and tetrahydrofuran. The cosolvents are necessary to impart porogen solubility.[137,138]

3.6. Directly Patterned Dielectrics in Four Process Steps

Low *k* dielectric films must be patterned prior to their integration into device structures. This is currently performed via subtractive processing, which involves a sequence of steps: a planar film is deposited, coated with a polymeric photoresist, followed by developing an image in the photosensitive layer with an aid of UV exposure and transferring the developed image into the underlayer by selective etching. The top layer of photosensitive film is then removed via wet cleaning or dry etching. Any damage to the electrical properties of the film during etching or photoresist removal must then be repaired to restore a low dielectric constant, often by exposure to a silane capping agent. Clearly, it would be advantageous to compress the number of steps required to produce a patterned film and approaches to this end have been suggested[139] In particular, replacing the subtractive scheme with an efficient additive process would have both economic and environmental advantages.

An enabling advantage of the SCF approach to ULK films is the ability to completely define the hierarchical structure in the template and then replicate into a metal oxide network by domain selective precursor condensation. Using this advantage, Nagarajan et al. developed a simple method to fabricate directly patterned mesoporous silicate films.[130,140,141] To produce the films, a photo acid generator (PAG) is added to the block copolymer template instead of the organic acid. Before performing domain selective precursor condensation, the templates are exposed to UV radiation through a photomask that has device scale features. Photolithographic exposure triggers generation of acid in the illuminated regions, which in turn leads to formation of a patterned silicate network upon infusion of Si alkoxides. (Here the strong acid generated from the PAG catalyzes silica condensation.) Because the acid generated in UV-exposed field segregate further into hydrophilic domains of the block copolymer, precursor condensation is controlled at the device level via the mask and domain level by the block copolymer morphology. Removal of the template by calcination yields a patterned mesoporous silicate film directly. This strategy does not require development of the exposed template or subsequent etching, as silica network formation is spatially defined in the film by the exposure. The resolution of the direct patterning process can be enhanced by using copolymer templates based on 248 or 193 nm chemically amplified resist platforms, and both positive and negative tone patterning is possible. Figure 15 shows a process schematic and the results for patterning of poly(styrene-*b*-*tert*-butyloxycarbonyloxystyrene). In another example, Nagarajan prepared directly patterned mesoporous silicate films using positive and negative tone strategies by performing phase selective silica condensation within lithographically exposed poly(styrene-*b*-*tert*-butyl acrlyate) (PS-*b*-PtbA) templates.[141] Template exposure through the mask triggers area selective generation of acid from the PAG, which in turn both deprotects the poly(*tert*-butyl acrlyate) block to yield a

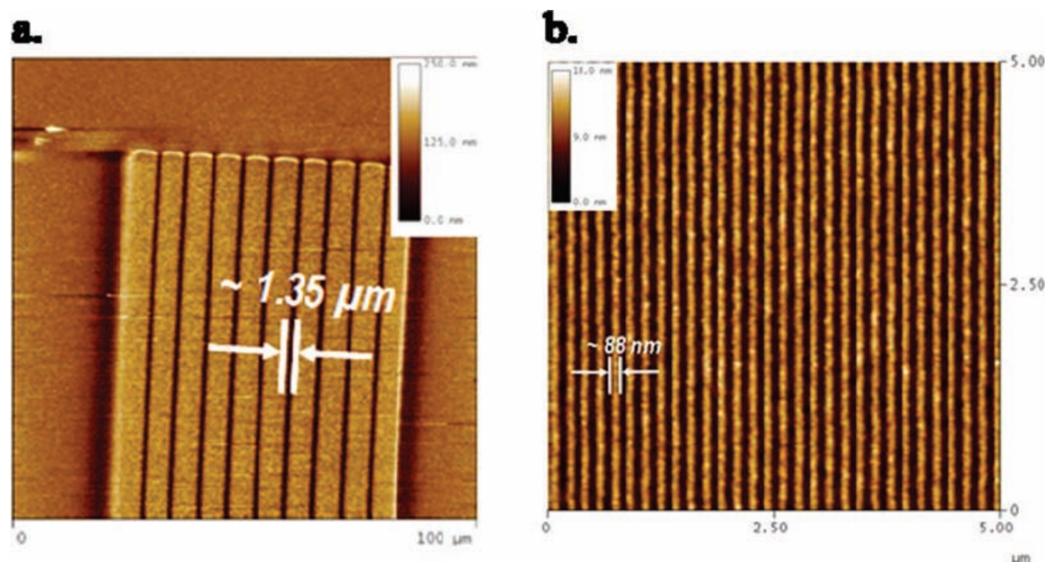

Figure 16. Calcined silica structure, synthesized through supercritical CO_2 infusion of tetraethyl ortho silicate (TEOS) into photo resist materials: (a) poly(*tert*-butyl methacrylate); (b) commercial off-the-shelf photoresist showing sub-100 nm structure.[141] Reprinted with permission from ref 141. Copyright 2009 Wiley-VCH.

poly(acrylic acid) block and provides a catalyst for silica precursor condensation. The ability of PS-*b*-PtbA to undergo chemical transformation in two stages, deprotection followed by cross-linking, enabled precise replications of the photomask in positive and negative tones. For positive tone replication, the regions exposed through the mask are cross-linked at elevated temperature, rendering them impermeable to the precursor in subsequent processing. The template was then flood exposed to activate the acid in the previously unexposed regions and infused with precursor, which permeated and then reacted in the uncross-linked domains only. Template removal via calcination yielded patterned mesoporous silicate films without etching.

The direct patterning procedure is quite general and can be applied to other templates including homopolymers that can be deprotected via chemical amplification and existing commercial resists. While templates that do not exhibit microphase segregation will not yield ordered mesopores, removal of the template will result in sub-1 nm porosity within the silicate films. The degree of porosity can be controlled by the loading of silica into the template prior to calcination. Figure 16a shows directly patterned lines produced by exposure, regioselective deprotection, and infusion of poly(*tert*-butyl methacrlyate) homopolymer. Recent unoptimized feasibility experiments using off-the-shelf 193 nm-line resists indicate that sub-100 nm resolution is readily achieved (Figure 12b), although optimization will be required to reduce line edge roughness. While these films will have lower porosities than their mesoporous counterparts (likely in the range of ~20%), the attainable dielectric constants should be acceptable for most device layers.

The potential for directly patterned films is greatly enhanced by the fact that a significant reduction in process steps provides an economic driver for implementation along with the potential for enhanced performance. The technology could potentially be implemented on a cost basis for larger device features in upper metallization layers using simple homopolymer templates. Microphase segregated templates to produce mesoporous films would not be required to achieve acceptable dielectric constants for upper metallization layers. Film structures and feature resolution could then be optimized prior to use for the smallest interconnect structure at the lowest levels. Moreover, the use of existing resist platforms as template materials has been demonstrated, which alleviates the need to qualify new materials for lithography. Finally, the tool design for the SCF infusion process is relatively simple and scaling to 200 mm wafers has been demonstrated.[123]

3.7. Surface Modification of Nanoporous Substrates

The low viscosity, absence of surface tension, and ease of removal of supercritical solutions render them ideal vehicles for carrying out chemistry on and within nanoporous solids. Future generations of semiconductor devices are expected to employ silicate-based ultralow-dielectric-constant films with significant volume fractions of sub-3-nm pores. The groups of Tripp and McCarthy have demonstrated that CO_2 is an excellent medium for surface modification via silylation chemistry.[142,143] Recent work by Muscat and Reidy have demonstrated that these chemistries can be adopted for the efficient surface modification of porous low *k* materials.[144-148] Xie et al. demonstrated that silylation of porous methylsilsesquioxane thin films using hexamethyldisilazane or trimethylchlorsilane significantly increased the hydrophobicity of the films, effectively repairing damage that occurred during exposure to oxygen ashing used in photoresist removal.[148] Pai et al. demonstrated the modification of mesoporous silicas prepared by the SCF assisted 3-D replication technique by reaction of surface silanols with silanes including using *n*-octyl trichlorosilane (OTCS) and *N*-methyl aminopropyltrimethoxysilanes.[124] Overall, surface modifications schemes in CO_2 are effective, easy to implement, and are a viable process option, particularly for porous nanostructured materials.

4. Conclusions

Supercritical fluids offer a combination of properties that are perhaps uniquely suited to the fabrication of devices with nanoscale features. The ability to conduct solution-based processing in an environment that, from a transport perspective, behaves more like a gas offers the possibility of hybrid approaches to deposition, etching, resist development, and

surface modification chemistries within the smallest device features. Conformal metal, metal oxide, and composite film formation via supercritical fluid deposition within challenging topographies at relatively high deposition rates are examples of this potential. The development of standard resists using CCS additives to CO_2 is another example.

Further opportunities are found in the 3-D replication of preorganized polymer templates organized at the nanoscale and patterned at the device scale to yield fully engineered silicate films that enable complete structural specifications of next-generation ultralow *k* and directly patterned dielectrics. In addition to providing access to well-ordered nanoporous media through the use of block copolymers, the ability to create directly patterned media using templates based on existing resist platforms currently in production provides a significant reduction in process steps and thus economic as well as technical advantages. Moreover, the demonstrated successful scaling of the three-dimensional replication approach to robust ULK films containing spherical pores on 200 mm process wafers indicates the viability of these processes.

Tools for high throughput wafer processing at supercritical conditions in the area of cleaning have been designed and constructed. This activity has resolved many of the technical and engineering challenges for integration of SCF process technologies and highlighted a few that need additional attention. This body of work from the design and tool communities provides a basis for moving forward.

So are opportunities for semiconductor device fabrication emerging or have they been missed? When viewed through the prism of the limited materials sets and the significant process integration challenges for the fabrication of interconnect structures for integrated circuits, the answer is not so clear. In the opinion of authors, the initial focus on wafer cleaning and photoresist stripping was unfortunate. These applications are among the most difficult fits for the intrinsic properties and solvent characteristics of supercritical carbon dioxide. In the end, the technology did not provide sufficient advantages over existing, lower cost techniques to justify adaptation. It is very possible that the failure of these efforts to reach successful commercialization despite significant investment may ultimately bias the industry away from future work in SCFs.

There are, however, significant opportunities that may overcome this hurdle. Single step Cu metallization, the development of direct patterning strategies for low *k* films, and the development of traditional resist systems with CCS salts are among them. In each case, the approach taken plays to the strengths of SCFs as solvents, operates at modest pressures with wide process windows, and offers technical advantages and in some cases offer the potential of substantial cost savings by eliminating or combining process steps.

It is intriguing to think of the possibilities if sustained SCF commercialization efforts had been initiated in one of these areas. Where would the field be now? For example Cu deposition via SFD appears to offer an end of the roadmap solution for single step metallization. By comparison, deposition of PVD Cu seed layers becomes increasingly difficult as interconnect dimensions decrease and work-arounds to remediate problems with PVD step coverage become more complex. With each generation, the potential advantages of SFD relative to existing process technology increase. Sustained development of SFD early on perhaps would have enabled insertion of a process tool as soon as the economic trade-off justified it. Such a development would then have provided a clear path for continued scaling—a successful tool would rapidly gain market share in this scenario. The reality of the current economic climate for semiconductors coupled with reduced emphasis on long-range research, capital investment in the existing tool base, and risk aversion likely precludes such a possibility for SCFs or for virtually any other "new" technology at this time. Without sustained development, it will be difficult to have the alternatives ready in time to avoid the costly investment in work-arounds. Eventually however even those work-around solutions may fail or become economically unfeasible. It may require such a cathartic failure in the scaling of an existing process to enable SCFs to get a "second look". A much more optimistic view is that the market will accept a technology that provides substantial cost savings through process compression; such a possibility exists for directly patterned dielectrics prepared by SCF or other routes.

While much of the work described in this review was motivated by the needs and size of the global semiconductor industry with specific emphasis on interconnect technology, the capabilities developed provide significant advantages for other applications in which there is greater freedom to implement new materials and process choices enabled by SCFs. These fields include MEMS, NEMS, sensors, alternative energy generation and storage, separations, micro/nanofluidics, and catalysis. In one example, we are employing the block copolymer 3-D replication technique to the design of cylindrical nanochannel arrays of precisely controlled diameter (see Figure 13b) for on-chip detection and separation schemes.[149] In another, the ability to sequentially deposit thin conformal metal and dielectric films in high-aspect-ratio structures offers a route to 3-D capacitor structures. The deposition of high quality wide band gap semiconductors[81] could enable applications to optoelectronics and other areas. We and others are employing SFD for deposition of pure and mixed catalyst systems.

A positive outcome for application of SCFs in a full scale fab environment may ultimately depend on a demonstrated success in a niche application outside of interconnect technologies. Such success would in turn lower the risk for development and implementation of similar technology in ICs. It will also depend critically on problem selection and the willingness of the semiconductor fab community to look at areas beyond wafer cleaning and stripping to those focused on device fabrication that are technically and economically compelling and in some cases easier to implement.

5. Acknowledgments

We gratefully acknowledge funding from the National Science Foundation through the Center for Hierarchical Manufacturing (CMMI-0531171) and CBET-0529034.

6. References

(1) McHugh, M.; Krukonis, V. *Supercritical Fluid Extraction*; Butterworth−Heinemann: Boston, 1993.
(2) O'Neil, A.; Watkins, J. J. *MRS Bull.* **2005**, *30*, 967.
(3) Hoggan, E. N.; Wang, K.; Flowers, D.; DeSimone, J. M.; Carbonell, R. G. *IEEE Trans. Semicond. Manuf.* **2004**, *17*, 510.
(4) Jones, C. A.; Zweber, A.; DeYoung, J. P.; McClain, J. B.; Carbonell, R.; DeSimone, J. M. *Crit. Rev. Solid State Mater. Sci.* **2004**, *29*, 97.
(5) King, J. W.; Williams, L. L. *Curr. Opin. Solid State Mater. Sci.* **2003**, *7*, 413.
(6) O'Neil, A.; Watkins, J. J. *Green Chem.* **2004**, *6*, 363.
(7) Weibel, G. L.; Ober, C. K. *Microelectron. Eng.* **2003**, *65*, 145.
(8) Zhang, X. G.; Johnston, K. P. *Chin. Sci. Bull.* **2007**, *52*, 27.

(9) Mount, D. J.; Rothman, L. B.; Robey, R. J. *Solid State Technol.* **2002**, *45*, 103.
(10) Aymonier, C.; Loppinet-Serani, A.; Reveron, H.; Garrabos, Y.; Cansell, F. *J. Supercrit. Fluids* **2006**, *38*, 242.
(11) Reverchon, E.; Adami, R. *J. Supercrit. Fluids* **2006**, *37*, 1.
(12) Cansell, F.; Aymonier, C.; Loppinet-Serani, A. *Curr. Opin. Solid State Mater. Sci.* **2003**, *7*, 331.
(13) Cooper, A. I. *J. Mater. Chem.* **2000**, *10*, 207.
(14) Darr, J. A.; Poliakoff, M. *Chem. Rev.* **1999**, *99*, 495.
(15) Cooper, A. I.; DeSimone, J. M. *Curr. Opin. Solid State Mater. Sci.* **1996**, *1*, 761.
(16) Savage, P. E.; Gopalan, S.; Mizan, T. I.; Martino, C. J.; Brock, E. E. *AIChE J.* **1995**, *41*, 1723.
(17) Cooper, A. I. *Adv. Mater.* **2003**, *15*, 1049.
(18) Tomasko, D. L.; Li, H. B.; Liu, D. H.; Han, X. M.; Wingert, M. J.; Lee, L. J.; Koelling, K. W. *Ind. Eng. Chem. Res.* **2003**, *42*, 6431.
(19) Linstrom, P. J.; Mallard, W. G. National Institute of Standards and Technology, Gaithersburg, MD, web site http://webbook.nist.gov.
(20) Zong, Y. F. Ph.D. Thesis, University of Massachusetts, 2005.
(21) Chandler, C. M.; Vogt, B. D.; Francis, T. J.; Watkins, J. J. *Macromolecules* , *42*, 4867.
(22) Wissinger, R. G.; Paulaitis, M. E. *J. Polym. Sci. Polym. Phys.* **1991**, *29*, 631.
(23) Wang, W.-C. V.; Kramer, E. J.; Sachse, W. H. *J. Polym. Sci., Part B: Polym. Phys.* **1982**, *20*, 1371.
(24) Gupta, R. R.; Ramachandra Rao, V. S.; Watkins, J. J. *Macromolecules* **2003**, *36*, 1295.
(25) Watkins, J. J.; McCarthy, T. J. *Macromolecules* **1995**, *28*, 4067.
(26) Kirby, C. F.; McHugh, M. A. *Chem. Rev.* **1999**, *99*, 565.
(27) Hansen, B. N.; Hybertson, B. M.; Barkley, R. M.; Sievers, R. E. *Chem. Mater.* **1992**, *4*, 749.
(28) Popov, V. K.; Bagratashvili, V. N.; Antonov, E. N.; Lemenovski, D. A. *Thin Solid Films* **1996**, *279*, 66.
(29) Blackburn, J. M.; Long, D. P.; Cabanas, A.; Watkins, J. J. *Science* **2001**, *294*, 141.
(30) Watkins, J. J.; McCarthy, T. J. U.S. Patent 5789027, 1998.
(31) Brissonneau, L.; Vahlas, C. *Chem. Vap. Deposition* **1999**, *5*, 135.
(32) Brissonneau, L.; de Caro, D.; Boursier, D.; Madar, R.; Vahlas, C. *Chem. Vap. Deposition* **1999**, *5*, 143.
(33) Karanikas, C. F.; Watkins, J. J. *Microelectron. Eng.* **2009**, DOI: 10.1016/j.mee.2009.08.011.
(34) Kondoh, E.; Fukuda, J. In 8th International Symposium on Supercritical Fluids, Kyoto, Japan, 2006; p 466.
(35) Zong, Y. F.; Watkins, J. J. In *21st Advanced Metallization Conference (AMC 2004), San Diego, CA*; Erb, D., Ramm, P., Masu, K., Osaki, A., Eds.; 2004; p 353.
(36) Cabanas, A.; Shan, X. Y.; Watkins, J. J. *Chem. Mater.* **2003**, *15*, 2910.
(37) Blackburn, J. M.; Long, D. P.; Watkins, J. J. *Chem. Mater.* **2000**, *12*, 2625.
(38) Hunde, E. T.; Watkins, J. J. *Chem. Mater.* **2004**, *16*, 498.
(39) Long, D. P.; Blackburn, J. M.; Watkins, J. J. *Adv. Mater.* **2000**, *12*, 913.
(40) Watkins, J. J.; Blackburn, J. M.; McCarthy, T. J. *Chem. Mater.* **1999**, *11*, 213.
(41) Cabanas, A.; Long, D. P.; Watkins, J. J. *Chem. Mater.* **2004**, *16*, 2028.
(42) O'Neil, A.; Watkins, J. J. *Chem. Mater.* **2006**, *18*, 5652.
(43) Kondoh, E. *Jpn. J. Appl. Phys., Part 1* **2004**, *43*, 3928.
(44) Erkey, C. *J. Supercrit. Fluids* **2009**, *47*, 517.
(45) Fernandes, N. E.; Fisher, S. M.; Poshusta, J. C.; Vlachos, D. G.; Tsapatsis, M.; Watkins, J. J. *Chem. Mater.* **2001**, *13*, 2023.
(46) Kondoh, E.; Shigama, K. *Thin Solid Films* **2005**, *491*, 228.
(47) Matsubara, M.; Hirose, M.; Tamai, K.; Shimogaki, Y.; Kondoh, E. *J. Electrochem. Soc.* **2009**, *156*, H443.
(48) Peng, Q.; Spagnola, J. C.; Parsons, G. N. *J. Electrochem. Soc.* **2008**, *155*, D580.
(49) Lin, C. S.; Lam, F. L. Y.; Hu, X. J.; Tam, W. Y.; Ng, K. M. *J. Phys. Chem. C* **2008**, *112*, 10068.
(50) Zhao, B.; Momose, T.; Ohkubo, T.; Shimogaki, Y. *Microelectron. Eng.* **2008**, *85*, 675.
(51) Tsang, C. Y.; Streett, W. B. *Chem. Eng. Sci.* **1981**, *36*, 993.
(52) Gurdial, G. S.; Foster, N. R.; Yun, S. L. J.; Tilly, K. D. *ACS Symp. Ser.* **1993**, *514*, 34.
(53) Zhu, H. G.; Tian, Y. L.; Chen, L.; Qin, Y.; Feng, J. J. *Chin. J. Chem. Eng.* **2001**, *9*, 322.
(54) Zong, Y. F.; Watkins, J. J. *Chem. Mater.* **2005**, *17*, 560.
(55) Kim, D. H.; Wentorf, R. H.; Gill, W. N. *J. Electrochem. Soc.* **1993**, *140*, 3267.
(56) Shan, X. Y.; Schmidt, D. P.; Watkins, J. J. *J. Supercrit. Fluids* **2007**, *40*, 84.
(57) Cabanas, A.; Blackburn, J. M.; Watkins, J. J. In European Workshop on Materials for Advanced Metallization, Vaals, The Netherlands, 2002; p 53.
(58) Momose, T.; Ohkubo, T.; Sugiyama, M.; Shimogaki, Y. *Thin Solid Films* **2008**, *517*, 674.
(59) Zong, Y. F.; Shan, X. Y.; Watkins, J. J. *Langmuir* **2004**, *20*, 9210.
(60) Karanikas, C. F.; Han, L.; Vlassak, J. J.; Watkins, J. J. *J. Eng. Mater. Technol.* **2009**, in press.
(61) Momose, T.; Sugiyama, M.; Shimogaki, Y. *Jpn. J. Appl. Phys.* **2008**, *47*, 885.
(62) Ritzdorf, T. In *Advanced Metallization Conference 2006, San Diego, CA*; Russell, S. W., Mills, M. E., Osaki, A., Yoda, T., Eds.; 2006; p 69.
(63) Blackburn, J. M. ; Gaynor, J.; Drewery, J.; Hunde, E.; Watkins, J. J. In *Advanced Metallization Conference 2003 (AMC 2003), Montreal*; Ray, G. W., Smy, T., Ohta, T., Tsujimura, M., Eds.; 2003; p 601.
(64) Watkins, J. J.; Blackburn, J. M.; Long, D. P.; Lazorcik, J. L. U.S. Patent 6689700, 2004.
(65) Ohde, H.; Kramer, S.; Moore, S.; Wai, C. M. *Chem. Mater.* **2004**, *16*, 4028.
(66) Ye, X. R.; Wai, C. M.; Zhang, D. Q.; Kranov, Y.; McIlroy, D. N.; Lin, Y. H.; Engelhard, M. *Chem. Mater.* **2003**, *15*, 83.
(67) Kim, J.; Taylor, D.; DeYoung, J.; McClain, J. B.; DeSimone, J. M.; Carbonell, R. G. *Chem. Mater.* **2009**, *21*, 913.
(68) Ramesh, R.; Aggarwal, S.; Auciello, O. *Mater. Sci. Eng., R* **2001**, *32*, 191.
(69) Oishi, N.; Atkinson, A.; Brandon, N. P.; Kilner, J. A.; Steele, B. C. H. *J. Am. Ceram. Soc.* **2005**, *88*, 1394.
(70) Trovarelli, A. *Catal. Rev.−Sci. Eng.* **1996**, *38*, 439.
(71) Kuomoto, K.; Terasaki, I.; Funahashi, R. *MRS Bull.* **2006**, *31*, 206.
(72) Tokura, Y.; Takagi, H.; Uchida, S. *Nature* **1989**, *337*, 345.
(73) Uchida, H.; Otsubo, A.; Itatani, K.; Koda, S. *Jpn. J. Appl. Phys., Part 1* **2005**, *44*, 1901.
(74) Gougousi, T.; Barua, D.; Young, E. D.; Parsons, G. N. *Chem. Mater.* **2005**, *17*, 5093.
(75) Gougousi, T.; Chen, Z. Y. *Thin Solid Films* **2008**, *516*, 6197.
(76) Peng, Q.; Hojo, D.; Park, K. J.; Parsons, G. N. *Thin Solid Films* **2008**, *516*, 4997.
(77) O'Neil, A.; Watkins, J. J. *Chem. Mater.* **2007**, *19*, 5460.
(78) Lee, J. H.; Son, J. Y.; Lee, H. B. R.; Lee, H. S.; Ma, D. J.; Lee, C. S.; Kim, H. J. *Electrochem. Solid-State Lett.* **2009**, *12*, D45.
(79) Tsai, C. T.; Chang, T. C.; Kin, K. T.; Liu, P. T.; Yang, P. Y.; Weng, C. F.; Huang, F. S. *J. Appl. Phys.* **2008**, 103.
(80) Tsai, C. T.; Chang, T. C.; Liu, P. T.; Cheng, Y. L.; Kin, K. T.; Huang, F. S. *Electrochem. Solid-State Lett.* **2009**, *12*, H35.
(81) Yang, J.; Hyde, J. R.; Wilson, J. W.; Mallik, K.; Sazio, P. J.; O'Brien, P.; Malik, M. A.; Afzaal, M.; Nguyen, C. Q.; George, M. W.; Howdle, S. M.; Smith, D. C. *Adv. Mater.* **2009**, *21*, 4115.
(82) Jessop, P. G. In *7th International Conference on Carbon Dioxide Utilization, Seoul, South Korea*; Park, S. E., Chang, J. S., Lee, K. W., Eds.; 2003, p 355.
(83) Jessop, P. G.; Subramaniam, B. *Chem. Rev.* **2007**, *107*, 2666.
(84) Xie, B.; Finstad, C. C.; Muscat, A. J. *Chem. Mater.* **2005**, *17*, 1753.
(85) Bae, J. H.; Alam, M. Z.; Jung, J. M.; Gal, Y. S.; Lee, H.; Kim, H. G.; Lim, K. T. In 10th Annual SEMATECH Surface Preparation and Cleaning Conference (SPCC), Austin, TX, 2008, p 128.
(86) Bessel, C. A.; Denison, G. M.; DeSimone, J. M.; DeYoung, J.; Gross, S.; Schauer, C. K.; Visintin, P. M. *J. Am. Chem. Soc.* **2003**, *125*, 4980.
(87) Dunbar, A.; Omiatek, D. M.; Thai, S. D.; Kendrex, C. E.; Grotzinger, L. L.; Boyko, W. J.; Weinstein, R. D.; Skaf, D. W.; Bessel, C. A.; Denison, G. M.; DeSimone, J. M. *Ind. Eng. Chem. Res.* **2006**, *45*, 8779.
(88) Shan, X. Y.; Watkins, J. J. *Thin Solid Films* **2006**, *496*, 412.
(89) Ventosa, C.; Rebiscoul, D.; Perrut, V.; Ivanova, V.; Renault, O.; Passemard, G. *Microelectron. Eng.* **2008**, *85*, 1629.
(90) Durando, M.; Morrish, R.; Muscat, A. J. *J. Am. Chem. Soc.* **2008**, *130*, 16659.
(91) Jones, C. A.; Yang, D. X.; Irene, E. A.; Gross, S. M.; Wagner, M.; DeYoung, J.; DeSimone, J. M. *Chem. Mater.* **2003**, *15*, 2867.
(92) Li, Y. X.; Yang, D.; Jones, C. A.; DeSimone, J. M.; Irene, E. A. *J. Vac. Sci. Technol., B* **2007**, *25*, 1139.
(93) Goldfarb, D. L.; de Pablo, J. J.; Nealey, P. F.; Simons, J. P.; Moreau, W. M.; Angelopoulos, M. *J. Vac. Sci. Technol., B* **2000**, *18*, 3313.
(94) Namatsu, H. *J. Photopolym. Sci. Technol.* **2002**, *15*, 381.
(95) Cotte, J. M.; Goldfarb, D. L.; McCullough, K. J.; Moreau, W. M.; Pope, K. R.; Simons, J. P.; Taft, C. J. (International Business Machines Corporation) U.S. Patent 6454869, 2002.
(96) Namatsu, H. In 45th International Conference on Electron, Ion, and Photon Beam Technology and Nanofabrication, Washington, DC, 2001, p 2709.

(97) Namatsu, H. In *Conference on Advances in Resist Technology and Processing XXI, Santa Clara, CA*; Sturtevant, J. L., Ed.; 2004; p 482.
(98) Lee, M. Y.; Do, K. M.; Ganapathy, H. S.; Lo, Y. S.; Kim, J. J.; Choi, S. J.; Lim, K. T. *J. Supercrit. Fluids* **2007**, *42*, 150.
(99) Sundararajan, N.; Yang, S.; Ogino, K.; Valiyaveettil, S.; Wang, J. G.; Zhou, X. Y.; Ober, C. K.; Obendorf, S. K.; Allen, R. D. *Chem. Mater.* **2000**, *12*, 41.
(100) Pham, V. Q.; Ferris, R. J.; Hamad, A.; Ober, C. K. *Chem. Mater.* **2003**, *15*, 4893.
(101) Flowers, D.; Hoggan, E. N.; Carbonell, R.; DeSimone, J. M. *Proc. SPIE* **2002**, *419*, 4690.
(102) Felix, N.; Ober, C. K. *Chem. Mater.* **2008**, *20*, 2932.
(103) Shiraishi, H.; Yamamoto, J.; Sakamizu, T. *J. Photopolym. Sci. Technol.* **2006**, *19*, 367.
(104) De Silva, A.; Felix, N. M.; Ober, C. K. *Adv. Mater.* **2008**, *20*, 3355.
(105) Felix, N. M.; De Silva, A.; Ober, C. K. *Adv. Mater.* **2008**, *20*, 1303.
(106) Wagner, M.; DeYoung, J.; Harbinson, C. In *Conference on Advances in Resist Technology and Processing XXIII, San Jose, CA*; Lin, Q., Ed.; 2006; p U603.
(107) Wagner, M.; DeYoung, J.; Harbinson, C.; Miles, M. In *Conference on Advances in Resist Technology and Processing XXIII, San Jose, CA*; Lin, Q., Ed.; 2006; p U1551.
(108) Tanaka, M.; Rastogi, A.; Toepperwein, G. N.; Riggleman, R. A.; Felix, N. M.; de Pablo, J. J.; Ober, C. K. *Chem. Mater.* **2009**, *21*, 3125.
(109) Zweber, A. E.; Wagner, M.; Carbonell, R. G. *J. Phys. Chem. B* **2009**, *113*, 9687.
(110) Zweber, A. E.; Wagner, M.; DeYoung, J.; Carbonell, R. G. *Langmuir* **2009**, *25*, 6176.
(111) Kim, S. H.; Yuvaraj, H.; Jeong, Y. T.; Park, C.; Kim, S. W.; Lim, K. T. *Microelectron. Eng.* **2009**, *86*, 171.
(112) Fan, H. Y.; Hartshorn, C.; Buchheit, T.; Tallant, D.; Assink, R.; Simpson, R.; Kisse, D. J.; Lacks, D. J.; Torquato, S.; Brinker, C. J. *Nat. Mater.* **2007**, *6*, 418.
(113) Gungor, M. R.; Watkins, J. J.; Maroudas, D. *Appl. Phys. Lett.* **2008**, *92*, 3.
(114) Bates, F. S.; Fredrickson, G. H. *Phys. Today* **1999**, *52*, 32.
(115) Hawker, C. J.; Russell, T. P. *MRS Bull.* **2005**, *30*, 952.
(116) Tirumala, V. R.; Romang, A.; Agarwal, S.; Lin, E. K.; Watkins, J. J. *Adv. Mater.* **2008**, *20*, 1603.
(117) Segalman, R. A.; Yokoyama, H.; Kramer, E. J. *Adv. Mater.* **2001**, *13*, 1152.
(118) Stoykovich, M. P.; Muller, M.; Kim, S. O.; Solak, H. H.; Edwards, E. W.; de Pablo, J. J.; Nealey, P. F. *Science* **2005**, *308*, 1442.
(119) Gupta, R. R.; Lavery, K. A.; Francis, T. J.; Webster, J. R. P.; Smith, G. S.; Russell, T. P.; Watkins, J. J. *Macromolecules* **2003**, *36*, 346.
(120) Vogt, B. D.; Brown, G. D.; Ramachandra Rao, V. S.; Watkins, J. J. *Macromolecules* **1999**, *32*, 7907.
(121) Vogt, B. D.; RamachandraRao, V. S.; Gupta, R. R.; Lavery, K. A.; Francis, T. J.; Russell, T. P.; Watkins, J. J. *Macromolecules* **2003**, *36*, 4029.
(122) Tanaka, S.; Hillhouse, H. W. *Chem. Lett.* **2006**, *35*, 928.
(123) Pai, R. A.; Humayun, R.; Schulberg, M. T.; Sengupta, A.; Sun, J. N.; Watkins, J. J. *Science* **2004**, *303*, 507.
(124) Pai, R. A.; Watkins, J. J. *Adv. Mater.* **2006**, *18*, 241.
(125) Tirumala, V. R.; Pai, R. A.; Agarwal, S.; Testa, J. J.; Bhatnagar, G.; Romang, A. H.; Chandler, C.; Gorman, B. P.; Jones, R. L.; Lin, E. K.; Watkins, J. J. *Chem. Mater.* **2007**, *19*, 5868.
(126) Geraud, D.; Magbitang, T.; Volksen, W.; Simonyi, E. E.; Miller, R. D. In *IEEE International Interconnect Technology Conference 2005*; IEEE: Burlingame, CA, 2005, p 226.
(127) Vogt, B. D.; Pai, R. A.; Lee, H. J.; Hedden, R. C.; Soles, C. L.; Wu, W. L.; Lin, E. K.; Bauer, B. J.; Watkins, J. J. *Chem. Mater.* **2005**, *17*, 1398.
(128) Li, X. X.; Vogt, B. D. *Chem. Mater.* **2008**, *20*, 3229.
(129) Li, X.; Song, L. Y.; Vogt, B. D. *J. Phys. Chem. C* **2008**, *112*, 53.
(130) Nagarajan, S.; Bosworth, J. K.; Ober, C. K.; Russell, T. P.; Watkins, J. J. *Chem. Mater.* **2008**, *20*, 604.
(131) Nagarajan, S.; Li, M. Q.; Pai, R. A.; Bosworth, J. K.; Busch, P.; Smilgies, D. M.; Ober, C. K.; Russell, T. P.; Watkins, J. J. *Adv. Mater.* **2008**, *20*, 246.
(132) Du, P.; Li, M. Q.; Douki, K.; Li, X. F.; Garcia, C. R. W.; Jain, A.; Smilgies, D. M.; Fetters, L. J.; Gruner, S. M.; Wiesner, U.; Ober, C. K. *Adv. Mater.* **2004**, *16*, 953.
(133) Gates, S. M.; Grill, A.; Dimitrakopoulos, C.; Restaino, D.; Lane, M.; Patel, V.; Cohen, S.; Simonyi, E.; Liniger, E.; Ostrovski, Y.; Augur, R.; Sherwood, M.; Klymko, N.; Molis, S.; Landers, W.; Edelstein, D.; Sankaran, S.; Wisnieff, R.; Ivers, T.; Yim, K.; Nguyen, V.; Nowak, T.; Rocha, J. C.; Reiter, S.; Demos, A. In *Advanced Metallization Conference 2006, San Diego, CA*; Russell, S. W., Mills, M. E., Osaki, A., Yoda, T., Eds.; 2006, p 351.
(134) Grill, A. *Annu. Rev. Mater. Res.* **2009**, *39*, 49.
(135) Berry, I. L.; Waldfried, C.; Durr, K. In *Symposium on Materials, Processes, Integration and Reliability in Advanced Interconnects for Micro- and Nanoelectronics, San Francisco, CA*; Lin, Q., Ryan, E. T., Wu, W., Yoon, D. Y., Eds.; 2007, p 15.
(136) Pai, R. A.; Watkins, J. J. 2006, unpublished data.
(137) Lubguban, A. A.; Lubguban, J. A.; Othman, M. T.; Shende, R. V.; Gangopadhyay, S.; Miller, R. D.; Volksen, W.; Kim, H. C. *Thin Solid Films* **2008**, *516*, 4733.
(138) Lubguban, J. A.; Gangopadhyay, S.; Lahlouh, B.; Rajagopalan, T.; Biswas, N.; Sun, J.; Huang, D. H.; Simon, S. L.; Mallikarjunan, A.; Kim, H. C.; Hedstrom, J.; Volksen, W.; Miller, R. D.; Toney, M. F. *J. Mater. Res.* **2004**, *19*, 3224.
(139) Schmid, G. M.; Stewart, M. D.; Wetzel, J.; Palmieri, F.; Hao, J. J.; Nishimura, Y.; Jen, K.; Kim, E. K.; Resnick, D. J.; Liddle, J. A.; Willson, C. G. *J. Vac. Sci. Technol., B* **2006**, *24*, 1283.
(140) Nagarajan, S.; Bosworth, J. K.; Ober, C. K.; Russell, T. P.; Watkins, J. J. In *24th Advanced Metallization Conference 2007 (AMC), Albany, NY*; McKerrow, A. J., ShachamDiamand, Y., Shingubara, S., Shimogaki, Y., Eds.; 2007, p 495.
(141) Nagarajan, S.; Russell, T. P.; Watkins, J. J. *Adv. Funct. Mater.* **2009**, *19*, 2728.
(142) Cao, C. T.; Fadeev, A. Y.; McCarthy, T. J. *Langmuir* **2001**, *17*, 757.
(143) Combes, J. R.; White, L. D.; Tripp, C. P. *Langmuir* **1999**, *15*, 7870.
(144) Gorman, B. P.; Orozco-Teran, R. A.; Zhang, Z.; Matz, P. D.; Mueller, D. W.; Reidy, R. F. *J. Vac. Sci. Technol., B* **2004**, *22*, 1210.
(145) Xie, B.; Choate, L.; Muscat, A. J. In 14th Biennial Conference on Insulating Films on Semiconductors, Leuven, Belgium, 2005, p 349.
(146) Xie, B.; Muscat, A. J. In European Workshop on Materials for Advanced Metallization (MAM2004), Brussels, Belgium, 2004, p 52.
(147) Xie, B.; Muscat, A. J. In European Workshop on Materials for Advanced Metallization, Dresden, Germany, 2005, p 434.
(148) Xie, B.; Muscat, A. J.; Busch, E.; Rhoad, T. In *21st Advanced Metallization Conference (AMC 2004), San Diego, CA*; Erb, D., Ramm, P., Masu, K., Osaki, A., Eds.; 2004; p 475.
(149) Chen, H. T.; Crosby, T. A.; Park, M. H.; Nagarajan, S.; Rotello, V. M.; Watkins, J. J. *Mater. Chem.* **2009**, *19*, 70.
(150) Rothman, L. Supercritical CO_2 Tools and Applications for Semiconductors. NSF/SRC Engineering Research Center for Environmentally Benign Semiconductor Manufacturing Annual Retreat, August 21−22, 2003; SC Fluids, Inc.: Nashua, NH, 2003; available at http://www.nsfstc.unc.edu/.
(151) Product Data DFP, 200-Dense Fluid Processor High-Precision Advanced Wafer Chamber; BOC Edwards: Wilmington, MA, 2002.

CR900255W